

AD-A107 246

ROCHESTER UNIV NY DEPT OF CHEMISTRY
LASER-STIMULATED MOLECULAR DYNAMICS AND RATE PROCESSES.(U)
NOV 81 T F GEORGE

F/G 20/5

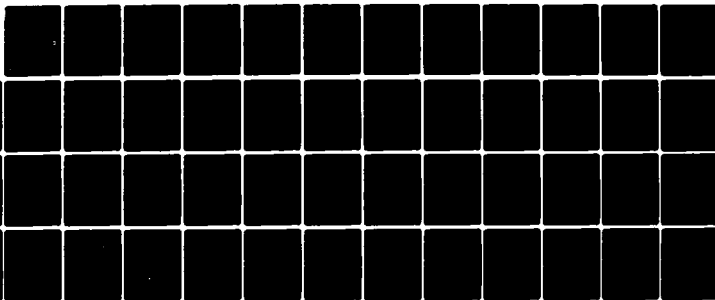
N00014-80-C-0472

UNCLASSIFIED

TR-14

NL

1 of 1
20/11/86



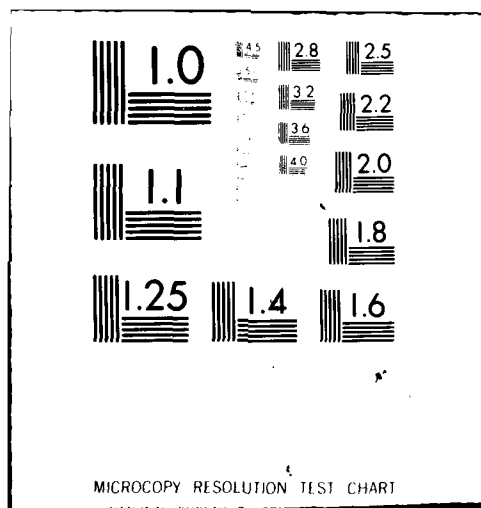
END

DATE

FILED

(2-8)

DTIC



LEVEL

(11)

OFFICE OF NAVAL RESEARCH

Contract N00014-80-C-0472

Task No. NR 056-749

TECHNICAL REPORT No. 14

Laser-Stimulated Molecular Dynamics and Rate Processes.

by

Thomas F. George

Prepared for Publication

in

The Journal of Physical Chemistry

University of Rochester
Department of Chemistry
Rochester, New York 14627

November, 1981

Reproduction in whole or in part is permitted for any purpose
of the United States Government.

This document has been approved for public release and sale;
its distribution is unlimited.

DTIC
SELECTE
NOV 10 1981

H

D

AD A107246

DTIC FILE COPY

Unclassified

SECURITY CLASSIFICATION OF THIS PAGE (When Data Entered)

REPORT DOCUMENTATION PAGE		READ INSTRUCTIONS BEFORE COMPLETING FORM
1. REPORT NUMBER 14	2. GOVT ACCESSION NO. AD-7107 246	3. RECIPIENT'S CATALOG NUMBER
4. TITLE (and Subtitle) LASER-STIMULATED MOLECULAR DYNAMICS AND RATE PROCESSES		5. TYPE OF REPORT & PERIOD COVERED Interim Technical Report
		6. PERFORMING ORG. REPORT NUMBER
7. AUTHOR(s) Thomas F. George		8. CONTRACT OR GRANT NUMBER(s) N00014-80-C-0472
9. PERFORMING ORGANIZATION NAME AND ADDRESS University of Rochester Department of Chemistry Rochester, New York 14627		10. PROGRAM ELEMENT, PROJECT, TASK AREA & WORK UNIT NUMBERS NR 056-749
11. CONTROLLING OFFICE NAME AND ADDRESS Office of Naval Research Chemistry Program Code 472 Arlington, Virginia 22217		12. REPORT DATE November 1981
		13. NUMBER OF PAGES 49
14. MONITORING AGENCY NAME & ADDRESS (if different from Controlling Office)		15. SECURITY CLASS. (of this report) Unclassified
		15a. DECLASSIFICATION/DOWNGRADING SCHEDULE
16. DISTRIBUTION STATEMENT (of this Report) This document has been approved for public release and sale; its distribution is unlimited.		
17. DISTRIBUTION STATEMENT (of this abstract entered in Block 20, if different from Report)		
18. SUPPLEMENTARY NOTES Prepared for publication in The Journal of Physical Chemistry, in press.		
19. KEY WORDS (Continue on reverse side if necessary and identify by block number) GAS-PHASE PROCESSES SURFACE PROCESSES ELECTRONIC-FIELD REPRESENTATION SELECTIVE EXCITATION ENERGY TRANSFER AND IONIZATION HETEROGENEOUS CATALYSIS EMISSION LINESHAPES MICROELECTRONICS TRANSITION STATE SPECTROSCOPY		
20. ABSTRACT (Continue on reverse side if necessary and identify by block number) A review of theoretical work by the author and collaborators and related experiments is presented for two segments of laser-induced chemistry: molecular dynamics and rate processes in the 1 st gas phase and 2 nd at a solid surface and gas-surface interface. For the gas phase, the focus is on situations where the radiation interacts directly with the dynamics to enhance or create new processes. The field of laser-surface chemistry is still undergoing a procedure of definition, and progress to date is discussed. Theoretical failures as well as successes are analyzed, and viewpoints are offered as to new directions for both theory and experiment.		

DD FORM 1 JAN 73 1473

Unclassified

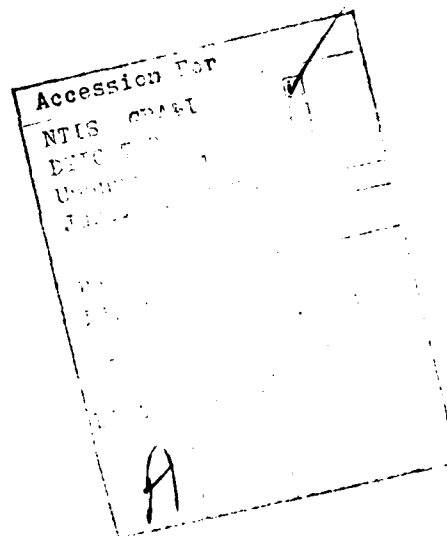
SECURITY CLASSIFICATION OF THIS PAGE (When Data Entered)

J. Phys. Chem. , in press

LASER-STIMULATED MOLECULAR DYNAMICS
AND RATE PROCESSES

Thomas F. George
Department of Chemistry
University of Rochester
Rochester, New York 14627

A review of theoretical work by the author and collaborators and related experiments is presented for two segments of laser-induced chemistry: molecular dynamics and rate processes in the 1) gas phase and 2) at a solid surface and gas-surface interface. For the gas phase, the focus is on situations where the radiation interacts directly with the dynamics to enhance or create new processes. The field of laser-surface chemistry is still undergoing a procedure of definition, and progress to date is discussed. Theoretical failures as well as successes are analyzed, and viewpoints are offered as to new directions for both theory and experiment.



Outline

- I. Introduction
- II. Gas-Phase Processes
 - A. General Concepts
 - 1. Photon Absorption "Time" (Rabi Flopping Time)
 - 2. Transition Dipoles
 - 3. Molecular Picture and Electronic-Field Representation
 - B. Examples
 - 1. Energy Transfer in Atom-Atom Collisions
 - 2. Energy Transfer in Molecule-Molecule Collisions
 - 3. Chemical Reactions
 - 4. Collisional Ionization
 - C. Pitfalls
 - 1. Potential Surface Shapes, Radiative Coupling and Collision Times
 - 2. No Net Absorption or Emission
 - 3. Very High Laser Intensities
 - D. New Directions
 - 1. Bound-Continuum Interactions
 - a. Spontaneous Emission
 - b. Chemi-Ionization
 - 2. Two Radiation Fields
 - a. Two Different Intense Lasers
 - b. Laser-Magnetic-Field Effects
 - c. Transition State Spectroscopy
- III. Surface Processes
 - A. General Concepts
 - B. Classes of Processes
 - 1. Nuclear Degrees of Freedom
 - 2. Electronic Degrees of Freedom
 - 3. Electronic-Nuclear Degrees of Freedom
 - C. Applications
 - 1. Heterogeneous Catalysis
 - 2. New Reaction Schemes
 - 3. Microelectronics

Acknowledgments

References

Figure Captions

I. Introduction

The general field of laser-induced chemistry is well established and growing quickly. The variety of chemical and physical processes (gas, liquid and solid) which have been probed, influenced or even created by laser radiation is vast.¹⁻⁴ Such processes have been reviewed in the past, and the purpose of this article is not to repeat the details found in Refs. 1-4 and other reviews available in the literature. Instead, we shall focus on two segments of laser-induced chemistry in which our research group has been working during the past six years.

The first segment is concerned with how intense laser radiation (power densities typically greater than a MW/cm^2 , although we shall mention cases involving lower power densities) might affect a molecular rate process by interacting directly with the dynamics of the nuclear and electronic motion. Review articles have appeared for both the experimental⁵ and theoretical⁵⁻⁷ aspects, and we have written a review of our own theoretical contributions as of three years ago⁸ (a brief review of more recent work forms part of a paper which also deals with nonradiative processes⁹). In light of these existing reviews, in this article we want to step back with a perspective and pick out several processes and calculations which best illustrate (in our opinion) the status of this field. We shall point out certain pitfalls and failures and then suggest new directions which might prove fruitful experimentally.

The second segment addresses the influence of more moderate laser radiation (power density generally less than a KW/cm^2) on molecular rate processes occurring at a solid surface, including heterogeneous processes at a gas-surface interface (although we shall also mention some processes involving intense radiation). This is a relatively new area of chemistry, and perhaps as much information is still passed on by word-of-mouth as in the open literature. We have written a review of our own theoretical contributions as of two years ago,¹⁰ and here we shall mention some main points of that

review, describe some ideas which we are currently pursuing and offer a perspective of this segment of laser-induced chemistry with regard to both basic and applied research.

II. Gas-Phase Processes

A. General Concepts

With sufficient intensity a laser can actually interact directly with the dynamics of a molecular rate process. This can be visualized by means of Fig. 1c depicting a chemical reaction between atom A and molecule BC, where the big circle denotes the interaction region. This should be contrasted with Fig. 1a, where the external radiation (with photon energy $\hbar\omega$) is resonant with energy levels of a reactant species, or with Fig. 1b, where the radiation ($\hbar\omega$) is not necessarily resonant with levels of individual reactants or products, and this feature offers a new flexibility in the use of lasers to influence chemical reactions. There are, however, constraints on this flexibility, some of which are now understood and others which are still being formulated. While this will be described in more detail in Part C of this section, we shall point out a few constraints here.

1. Photon Absorption "Time" (Rabi Flopping Time)

Resonant processes require lower laser intensities than nonresonant processes, and although the external radiation in Fig. 1c is not resonant with the levels of the individual reactants or products, the chances of the radiation influencing the dynamics of the A+BC collision are enhanced if some sort of resonance occurs during the collision. In this sense it is useful to construct adiabatic energy levels parametrized by nuclear coordinates, where the laser then comes into resonance at some point (or line or surface) between two such levels during the course of a nuclear "trajectory." Labelling the dipole operator by μ and the two electronic levels by i and j , we can express the transition dipole matrix as $\langle j | \mu | i \rangle$, and the strength of the interaction between the molecular system and the laser is given by

$$d_{ij} = E \langle j | \hat{\mu} | i \rangle, \quad (1)$$

where E is the electric field strength. [Strictly speaking, $\hat{\mu}$ and E are vectors, so that Eq. (1) represents a dot product.] The Rabi precession frequency associated with the transition between levels i and j is simply d_{ij}/\hbar . This frequency gives us a handle on the "time" it takes to absorb a photon, and the greater (lesser) the intensity, the less (greater) the time.

To be more quantitative, for a value of $\langle j | \hat{\mu} | i \rangle$ of one atomic unit (1 a.u. = $1 e a_0 = 2.54177$ Debyes; 1 Debye = 10^{-18} esu cm), d_{ij} has values of 0.002 cm^{-1} , 0.6 cm^{-1} , 20 cm^{-1} and 600 cm^{-1} for laser intensities of 1 KW/cm^2 , 1 MW/cm^2 , 1 GW/cm^2 and 1 TW/cm^2 , respectively. The corresponding "times" for photon absorption (i.e., $\hbar/2d_{ij}$, strictly known as the Rabi flopping time) are 1.25×10^{-10} sec, 5.0×10^{-12} sec, 1.25×10^{-13} sec and 5.0×10^{-15} sec, respectively. For a typical collision time of 10^{-13} to 10^{-12} sec, it is clear that intensities of excess of 1 MW/cm^2 are required (although in Part D of this section we shall discuss situations where the intensity can be as low as 1 KW/cm^2).

2. Transition Dipoles

From the above arguments we see that the size of the transition dipole plays a major role in the success of the laser-induced process, and this implies that one should look for electronic resonances whenever possible rather than vibrational/rotational resonances. Let us offer a few diatomic examples in support of this statement. Consider the HF molecule in its ground electronic state, $X^1\Sigma^+$, and the transition dipole matrix element $\langle j | \mu | i \rangle$ where μ is the dipole moment, i.e., the diagonal matrix element of $\hat{\mu}$ with respect to electronic degrees of freedom, and i and j refer to vibrational levels (ignoring rotations). Some values of this element in Debyes are:¹¹ $\langle 1 | \mu | 0 \rangle = 9.85 \times 10^{-2}$, $\langle 2 | \mu | 1 \rangle = 0.103$, $\langle 3 | \mu | 2 \rangle = 0.1115$, $\langle 2 | \mu | 0 \rangle = -1.25 \times 10^{-2}$ and $\langle 3 | \mu | 1 \rangle = -3.23 \times 10^{-2}$. The electronic transition dipole from the $X^1\Sigma^+$ state to the $1^1\Pi$ state is higher by an order of magnitude, having a value around 0.87 Debye at the equilibrium internuclear separation (0.92 \AA) and a

value of 1.3 Debyes at a separation of 0.53 \AA .¹² For CO in its ground electronic state, $X^1\Sigma^+$, some values of the transition dipole between both vibrational (first integer) and rotational (second integer) states in Debyes are:¹³ $\langle 20|\mu|00\rangle = -6.43 \times 10^{-3}$, $\langle 59|\mu|4,10\rangle = 0.238$ and $\langle 87|\mu|78\rangle = 0.295$. The electronic transition dipole from $X^1\Sigma^+$ to $A^1\Pi$ has a value of 2.0 Debyes,¹³ and from $a^3\Pi$ to $e^3\Sigma^-$ it has a value of 1.27 Debyes.¹⁴ For the XeF molecule, the dipole moment of the excited excimer state, $2^2\Sigma^+$, at equilibrium separation is -1.2 Debyes, which is probably an order of magnitude greater than the vibrational transition dipoles in that state, and the electronic transition dipole to the ground state, $1^2\Sigma^+$, is 3.7 Debyes at equilibrium separation.¹⁵ Finally, the NaXe molecule in its ground electronic state, $X^2\Sigma^+$, has a dipole moment of 2.4 Debyes and 0.16 Debye at internuclear separations of 3.0 \AA and 5.3 \AA , respectively, and the corresponding electronic transition dipoles to the $B^2\Sigma^+$ state are 6.2 Debyes and 6.7 Debyes.^{16,17} We should point out that the diagonal vibrational matrix element (vibrationally averaged dipole moment) can be comparable to or even greater than the electronic transition dipole; e.g., for $HF(X^1\Sigma^+)$, $\langle 0|\mu|0\rangle = 1.83$ Debyes. However, this has a much less significant influence on laser-induced vibrational transitions from $v=0$ to $v=1$ than $\langle 1|\mu|0\rangle$, and in general plays a small role except at very high laser intensities, such as near 1 TW/cm^2 .

We therefore realize that it is better to look for situations where laser photons come into resonance between electronic (or vibronic) potential energy curves or surfaces of a molecular collision system than between vibrationally adiabatic curves or surfaces associated with the same electronic state. This is especially important when the diatomic molecule of interest is homonuclear, say in an $A + BB$ collision. By symmetry, all vibrational matrix elements $\langle i|\mu|j\rangle$ for BB are identically zero since μ is zero, and while A can induce a dipole moment in BB , the laser intensity required for the situation denoted by Fig. 1c is generally greater for consideration of nuclear degrees of freedom alone than for both nuclear and electronic degrees of freedom, i.e., electronic transition dipoles.

3. Molecular Picture and Electronic-Field Representation

There are two general ways of viewing and consequently analyzing the situation of Fig. 1c, and for simplicity let us restrict ourselves to an atom-atom (A+B) collision system. The first way is known as the "atomic picture", which is appropriate when the laser is resonant or slightly off-resonant with two atomic levels, i.e., two levels of A, two levels of B or a level from each atom. When the laser is off-resonant, say with two levels of B, the relative motion of A can be viewed as perturbing these atomic levels and "tunes" them into resonance with the laser. The second way is the "molecular picture", whereby we view the levels of the A-B quasimolecule as coming into resonance with the laser. While the molecular picture is more general, the atomic picture can often be more convenient, particularly when the laser is near-resonant with levels of A or B or with molecular levels of A+B at asymptotic separation. For situations where the laser is far from resonance with asymptotic levels or where the resonance occurs in the interaction region of a chemical reaction (e.g., $A + BC \rightarrow AB + C$), the molecular picture is necessary. We shall adopt the molecular picture for purposes of illustration in this article, bearing in mind that it is sometimes more convenient (and appropriate) to use the atomic picture.

As a brief introduction to the molecular picture, we consider two field-free (without laser) potential energy curves of an A + B collision system, W_1 and W_2 , as functions of the internuclear separation, R . In Fig. 2a the vertical line corresponds to a laser photon in resonance between the two curves at the point $R = R_0$, where we can now view W_1 as shifted up in energy by $\hbar\omega$ to intersect W_2 at R_0 . To complete the picture, we must include radiative coupling, d_{12} [see Eq. (1)], which results in two new curves, E_1 and E_2 in Fig. 2b, with an avoided crossing at R_0 . As the laser intensity increases, the avoided crossing becomes larger. E_1 and E_2 are known as dressed levels¹⁸ or electronic-field levels.¹⁹

A more general picture is offered by Fig. 3, where N is a photon number (i.e., the number of photons in the field), and E_2 and E_3 correspond to E_1 and E_2 , respectively, in Fig. 2b for $N=1$. [Since the shapes of the electronic field levels with respect to R are independent of N , it is convenient to set N equal to one.] The four electronic-field levels correspond to the eigenvalues of the matrix

$$\begin{pmatrix} W_1 + N\hbar\omega & d & d_{11} & 0 \\ d & W_2 + (N-1)\hbar\omega & 0 & d_{22} \\ \hline d_{11} & 0 & W_1 + (N-1)\hbar\omega & d \\ 0 & d_{22} & d & W_2 + (N-2)\hbar\omega \end{pmatrix} \quad (2)$$

[$d \equiv d_{12} = d_{21}$ from Eq. (1), assuming real functions].

If we restrict ourselves to just the upper left 2×2 block, this is equivalent to making the rotating-wave approximation (RWA),²⁰ and the two eigenvalues are approximations for E_2 and E_3 . Of course, the block is automatically decoupled from the lower right block (which gives E_0 and E_1) in the case of a homonuclear diatomic molecule, since the dipole moments of the two electronic states, d_{11} and d_{22} , are zero. The forms of E_0 , E_1 , E_2 and E_3 under this block diagonalization are simply (for $N=1$)

$$E_0 = W_1 - \delta/2 - \Delta \quad (3a)$$

$$E_1 = W_1 + \delta/2 \quad (3b)$$

$$E_2 = W_2 - \delta/2 \quad (3c)$$

$$E_3 = W_2 + \delta/2 + \Delta, \quad (3d)$$

where $\Delta \equiv W_1 + \hbar\omega - W_2$ is the detuning and $\delta \equiv \sqrt{\Delta^2 + 4d^2} - \Delta$ is called the ac Stark shift (both Δ and δ are R -dependent quantities). While the inclusion of d_{11} and d_{22} can modify the dynamics,²¹ for single-photon absorption (or stimulated emission) it is usually a reasonable approximation to ignore virtual photon states and work with just the

upper left block, unless the laser intensity is very high. [Exceptions occur when we consider spontaneous emission, as depicted by the vertical lines in Fig. 3 and addressed in Part D.1.a. of this section.] We should point out that the matrix (2) results from a time-independent Schrödinger treatment.^{22,23} Within a time-dependent treatment,²⁴ the RWA involves discarding highly oscillatory terms and results in the same upper left block.

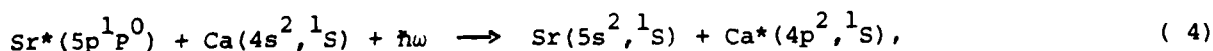
As a final comment in connection with Figs. 2 and 3, these can be viewed for a three-body A + BC system by regarding R as a translational or reaction coordinate, with the remaining coordinate(s) perpendicular to the page of the figure. In this sense the laser photon can be in resonance along a line in nuclear coordinate space (coming out of the page). Here the resonance interaction time between the molecular levels and the laser could be longer than for the case where the resonance occurs only at a single point, which would then be more favorable for laser-induced effects.

B. Examples.

The amount of theoretical work in this area, dating back a decade and reviewed in Refs. 5-7, far outweighs the experimental work to date. Nevertheless, the available experimental results are exciting and provide definite proof of the ideas represented by Fig. 1c. We shall mention some of these results, beginning with energy transfer in atom-atom collisions and diatom-diatom collisions, passing on to chemical reactions, then collisional ionization, and ending with electron-atom collisions. We shall intersperse a few of our own theoretical results, although our results will be utilized more in Part C.

1. Energy Transfer in Atom-Atom Collisions

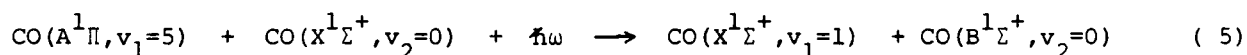
The first clean demonstration that laser radiation can interact with collision dynamics was carried out in a cell for the single-photon absorption energy transfer process²⁵



where $\hbar\omega$ is provided by a dye laser operating at 4977 \AA such that $\hbar\omega$ matches the asymptotic energy difference between the two molecular states correlating to Sr^*, Ca and Sr, Ca^* . This is a fine example of cooperative collisional and optical pumping, since the collision alone does not populate Ca^* , and the laser alone does not excite $\text{Ca}(^1\text{S})$ to $\text{Ca}^*(^1\text{S})$ due to no parity change. It is important to realize that $\hbar\omega$ matches the energy difference between molecular states rather than individual atomic states. More refined results along these lines were obtained for $\text{Eu} + \text{Sr}$ collisions, with resolution of various $^8\text{P}_J$ levels associated with Eu .²⁶ The laser intensities ranged from a MW/cm^2 to a GW/cm^2 . The atomic picture is suitable for describing these $\text{Sr} + \text{Ca}$ and $\text{Eu} + \text{Sr}$ processes, where the interaction of the radiation with the molecular system occurs at long range where the atomic levels are perturbed only slightly. A key reason for the success of these processes is that the laser interaction occurs over a long "time" in the near-asymptotic region where the molecular potentials are changing only slightly. We shall emphasize the importance of this in Part C.1.

2. Energy Transfer in Molecule-Molecule Collisions

The extension to diatom-diatom collisions was recently reported for the $\text{CO} + \text{CO}$ system, where one of the processes observed is²⁷

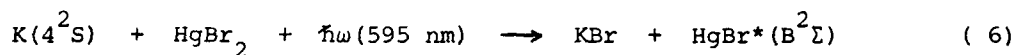


which involves the transfer of both electronic and vibrational energy transfer between CO molecules. A first laser creates CO in a rovibronic level ($v=5, J=12$) of the $A^1\Pi$ state via two-photon absorption, while a second laser (nonresonant with levels of CO) prepares a dressed or electronic-field state which can transfer its energy to $\text{CO}(X^1\Sigma^+, v_2=0)$ if it simultaneously makes a collision. Cross sections $> 10^{-16} \text{ cm}^2$ were obtained for an intensity of the second laser of $8 \text{ GW}/\text{cm}^2$.

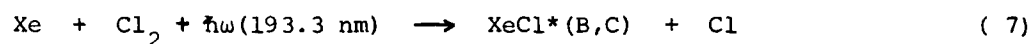
3. Chemical Reactions.

Ultimately the chemist is concerned with chemical reactions, and two splendid examples have been provided. The first is a crossed-beam experiment (two molec-

ular beams and a laser beam) for the process²⁸



where $h\nu$ from a dye laser (intensity $\sim \text{MW}/\text{cm}^2$) is nonresonant with any levels of the reactants or products. Emission from HgBr^* at 500 nm was observed only when the laser is on, so that this is an example of a laser-induced reaction to form an excited electronic state of a product which is inaccessible without the laser. The second example is a cell experiment on the process²⁹



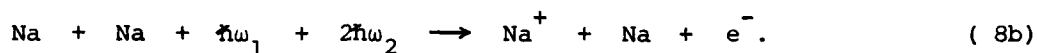
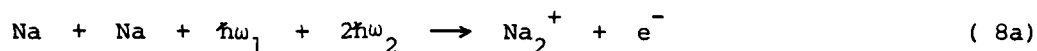
where $h\nu$ is provided by an ArF laser. Emission from the B and C states of XeCl was observed only when the ArF laser was on.

In both of the above examples, the laser evidently comes into resonance between the ground potential energy surface and the excited surfaces correlating to the excited product states. However, there appear to be strong differences between the two examples. K reacts with HgBr_2 to form HgBr in its ground electronic state in the absence of the laser, where the reaction is known to proceed through the formation of a long-lived complex.³⁰ Therefore one might view (6) more as a laser pumping the K-HgBr_2 quasimolecule rather than interacting to a large extent with the collision dynamics. For the case of (7), the ground electronic state of XeCl_2 lies about 1.8 eV above the $\text{Xe} + \text{Cl}_2$ asymptote,³¹ implying a sizeable barrier to reactive $\text{Xe} + \text{Cl}_2$ collision. This suggests that the laser is interacting with the collision dynamics to enhance or even cause the reaction as a whole, whether or not we are looking for XeCl^* or XeCl . It is possible that the photon absorption process tends to lengthen the time of collision, i.e., a XeCl_2 complex might be formed via photon absorption which then dissociates to $\text{XeCl}^* + \text{Cl}$.

4. Collisional Ionization

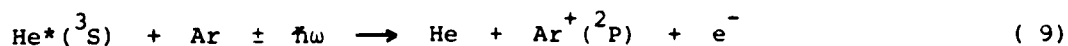
Several definitive experiments have been performed on the collisions of alkali atoms in the presence of various lasers, both under molecular beam conditions³²

and in a cell,³³ and on Sr + Cs collisions in a cell.³⁴ In one of the molecular beam experiments on alkali-alkali collisions, two Na beams were crossed with two lasers ($\hbar\omega_1$ and $\hbar\omega_2$) to result in the processes³²



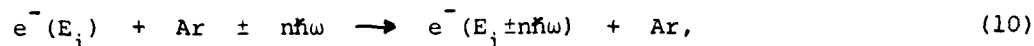
$\hbar\omega_1$ was fixed on resonance with the $3^2S \rightarrow 3^2P$ atomic transition while $\hbar\omega_2$ was varied from $16,121 \text{ cm}^{-1}$ to $17,321 \text{ cm}^{-1}$ (with an intensity around 10 MW/cm^2). While the spectra of Na_2^+ (associative ionization) and Na^+ are peaked at the values of $\hbar\omega_2$ corresponding to two-photon ($2\hbar\omega_2$) atomic resonances, there is considerable structure in the spectra between the peaks, corresponding to two-photon transitions into the electronic continuum. One can view the first $\hbar\omega_2$ photon either as "resonant" with a virtual atomic state³⁵ or as resonant with two excited-state molecular potentials of the Na-Na system.³⁶ The second photon then couples a discrete state with the electronic continuum. This is an important feature of laser-induced collisional ionization, since we are no longer locked into the picture of Fig. 2 showing a localized resonance configuration. The "resonance" of the photon between bound and continuum states can occur over a wide, continuous range of nuclear coordinates, which is favorable for laser-collision interactions.³⁷

Reaction (8b) represents a laser-assisted Penning ionization process, where collisional ionization does not occur in the absence of the laser. It is interesting to also consider laser-modified Penning ionization, where collisional ionization does occur without the laser, and an example has been provided by a theoretical calculation performed in our laboratory for the process³⁸



The energy spectrum of the emitted electron shows three peaks for a single-photon process. The central peak due to Coulomb coupling corresponds to ionization without the laser. The peaks on either side, separated in energy by $2\hbar\omega$, result from radiative bound-continuum coupling, where the peak lower in energy corresponds to stimulated photon emission while the higher peak corresponds to absorption.

While (9) has not yet been observed experimentally, support for this idea comes from experiments on electron-atom collisions in the presence of a CO₂ laser,³⁹



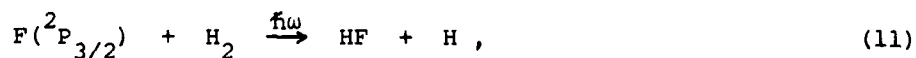
where E_i is the initial energy of the colliding electron. The energy spectrum of the scattered electron shows well-defined peaks each separated by $\hbar\omega$, where n as high as 3 was observed.

C. Pitfalls

After performing calculations on a variety of physical processes, we have gained some understanding of the unfavorable conditions for the situation depicted in Fig. 1c. We have just mentioned systems with favorable conditions in Part B, and here we shall draw on the results of some of our own work to point out pitfalls which should be avoided or carefully considered by both experimentalists and theorists.

1. Potential Surface Shapes, Radiative Coupling and Collision Times

The first pitfall is associated with the relative times of collision and photon absorption (strictly speaking, the Rabi flopping time in the latter case), alluded to earlier in Part A.1. As the collision time increases, the required Rabi precession frequency d_{ij}/\hbar [see Eq. (1)] and hence the required laser intensity decreases. This fact was important in the success of the energy transfer experiments reported in Refs. 25 and 26, where the laser photon is near-resonant with potential energy curves for a long range of the internuclear separation. The opposite situation occurs for the $F + H_2$ reaction in the presence of a Nd:glass laser,



as shown schematically in Fig. 4 where two potential energy surfaces are sketched along a reaction coordinate, s . The lower surface correlates from $F(^2P_{3/2}) + H_2$ to $HF(^1\Sigma^+) + H$ and the upper surface from $F^*(^2P_{1/2}) + H_2$ to $HF(^1,^3\Pi) + H$, where $HF(^1,^3\Pi)$ is inaccessible for energies of chemical interest (<5 eV). The photon comes into resonance with the surfaces in the exit valley as the products are receding from each other. There are two disadvantages to this: First, the difference between the slopes of W_1 and W_2 , $\Delta W' =$

$|dW_2/ds - dW_1/ds|$, is very large, and a simple inspection of the Landau-Zener-like formula for a local transition probability between the surfaces [see Appendix B in Ref. 24],

$$p = \exp[-\pi d_{12}^2 / (2v\hbar\Delta W')], \quad (12)$$

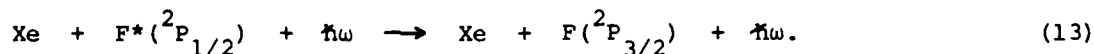
where d_{12} is given by Eq. (1) and v is the relative nuclear velocity, shows that this is unfavorable for strong dynamic transitions via radiative coupling. Second, the products are separating very rapidly due to the large exoergicity (~ 1 eV). In fact, for a typical classical trajectory three quarters of the total time is spent up to the saddle-point region, with only a quarter of the time in the exit valley. This leaves little "time" for strong interaction with the radiation field. As a result, semiclassical calculations show that the laser intensity must be increased beyond a TW/cm^2 before interesting effects occur, namely, where the branching ratio $\text{HF}(v=3)/\text{HF}(v=2)$ becomes greater than unity (it is less than unity in the absence of the laser).⁴⁰ Even though we are capitalizing on an electronic transition dipole, we have no advantage over a process which depends solely on vibrational dipoles.⁴¹

The most obvious remedy is to decrease the frequency of the laser so that the resonance occurs closer to the saddle-point region, where the slope difference is smaller and the nuclei are moving more slowly. This has been tried, computationally, and indeed the threshold intensity for laser-induced effects goes down by two orders of magnitude.⁴² A useful way to understand how the electronic transition dipole operates is to view the H product atom as serving to tune the 1Π and $1\Sigma^+$ labels of HF down into resonance with the photon, so that radiative coupling is essentially dominated by the strong electric dipole transition between these levels. As we back up around the saddle point, the strength of this electric dipole coupling decreases exponentially to zero, so one cannot reduce the photon frequency too much. For example, a CO_2 laser photon ($\hbar\omega=0.117$ eV) would come into resonance in the reactant region where the electric dipole coupling is zero and the radiative coupling is essentially magnetic dipole. However, magnetic dipole coupling is

typically two or more orders of magnitude less than electric dipole; for the $^2P_{3/2} \rightarrow ^2P_{1/2}$ spin-orbit transition it is only 0.008 a.u.⁴³ Further discussion on the favorable conditions for the process on Fig. 1c in terms of the features of shapes of potential energy surfaces and radiative coupling can be found in Ref. 44, which uses the reaction $\text{Li} + \text{HF} \rightarrow \text{LiF} + \text{H}$ as an example.

2. No Net Absorption or Emission

The term "photon catalysis" has been suggested for processes involving no net absorption (or emission) of photons.⁴⁵ While this represents an exciting prospect, such a process often requires far too high laser intensities to be feasible. In fact, the $\text{F} + \text{H}_2$ example provided in the previous two paragraphs involves no net photon adsorption, which is why $\hbar\omega$ is written above the arrow in (11) rather than on the same line as the reactants, and why the vertical arrow in Fig. 4 is double-ended. The laser simply serves to mix or couple the upper surface with the lower surface along a small portion of a trajectory. This is a second-order effect, which by definition has a lower probability than a first-order effect such as actual photon absorption (net photon absorption leads back to reactants). A clearer way to demonstrate the nature of this second-order effect is to consider the quenching of $\text{F}^*(^2P_{1/2})$ by collision with Xe in the presence of the 248-nm light of the KrF laser,



A classical-like interpretation (see Fig. 5) is that Xe and F approach each other on an excited covalent potential curve, up to the point where $\hbar\omega$ is resonant with this curve and an excimer curve correlating to $\text{Xe}^+ + \text{F}^-$, so that the system absorbs a photon (vertical arrow pointing up). The system then proceeds on the excimer curve until the energy difference between this curve and the ground-state covalent curve is $\hbar\omega$, at which point there is stimulated emission of a photon (vertical arrow pointing down). This stimulated Raman-like two-photon process is second-order, and as a result fully quantum mechanical calculations show that the quenching process is enhanced by the KrF laser only for intensities on the order of 10 GW/cm^2 or higher. The lesson to be learned is that whenever

possible, one should choose a process involving net photon absorption (or emission). There are, nevertheless, situations where second-order processes can be made to look more like first-order processes,^{7,9,45} and this will be discussed in Part D.2.c of this section.

As a final comment, the expense to set up the laser(s) is the same whether or not there is net photon absorption. The prospect of capturing and re-using photons in a situation where there is no net absorption is not yet well defined, either in terms of the procedure or the cost.

3. Very High Laser Intensities

In general, one should try to work with processes requiring as low a laser intensity as possible. A possible source of worry for experiments conducted in cells is gas breakdown (much less so for beam experiments),⁴⁶ although for reasonable pressures (<100 torr) we would expect that the laser intensity would have to be well beyond 100 GW/cm^2 before breakdown occurs.⁴⁷ Although this problem can be abrogated, one should worry about competing processes occurring in the presence of intense radiation, e.g., stimulated Brillouin scattering, blooming, self-focusing, etc., which could mask the process of interest. To a certain extent some of these stimulated processes, which sometimes occur primarily in the forward direction defined by the radiation propagation vector, might be avoided by making measurements away from this direction, e.g., placing a photodetector at 90° to the laser beam if fluorescence is being measured. In any event, higher intensities tend to increase the number of competing processes which might camouflage (or even preempt) the process of interest.

Laser characteristics become more critical in a theoretical study as the intensity increases. Throughout most of our calculations we have made a single-mode approximation for the radiation field. Model studies comparing results for single-mode, two-mode and ten-mode-locked lasers have shown this to be an accurate approximation provided the laser intensity is $\leq 10 \text{ GW/cm}^2$.⁴⁸ The explicit consideration of the coupling of photon angular momentum with the molecular angular momentum

makes a quantum mechanical treatment intractable, but model studies have shown that most of the complexities associated with this problem can be safely ignored or easily approximated provided the laser intensity is $\leq 100 \text{ GW/cm}^2$.⁴⁹

D. New Directions

1. Bound-Continuum Interactions

There are a variety of interesting experimental measurements and theoretical studies which can be carried out for processes involving bound-continuum interactions, i.e., coupling between a bound molecular state and a continuum. We shall address two such processes here: spontaneous emission and chemi-ionization.

a. Spontaneous Emission

A collision system can in principle emit photons in a continuous range of frequencies by means of coupling to a vacuum field. This can occur with or without an external laser field present, and for the moment let us consider the situation where the external field is absent. Within a Franck-Condon-type approximation, one can regard the molecular collision system in terms of a classical trajectory propagating on an excited-state potential surface. It can emit a photon of frequency ω at some point R in nuclear configuration space, where $\hbar\omega$ equals the energy difference at R_0 between the excited and ground-state surfaces, W_2 and W_1 , respectively. We can envision shifting W_2 down in energy by $\hbar\omega$ to cross W_1 at R_0 (analogous to Fig. 2). The resulting electronic-field curves exhibit an avoided crossing brought about by radiative coupling to the vacuum field, and a transition from E_2 to E_1 corresponds to no photon emission. The probability, p , of the transition is given by Eq. (12), except now d_{12} represents the radiative coupling to the vacuum field. Of course, at a previous point infinitesimally close to R_0 , the system also did not emit a photon, and in fact, up to R_0 we have a "continuous" product of p -factors for not emitting a photon.⁵⁰ This product, known as a pre-emission loss probability, can be represented in terms of an integral up to R_0 :

$$\Pi p = \exp \left[- \int_0^{R_0} dR \phi(R) \right], \quad (14)$$

where

$$\phi(R) = \pi d_{12}^2 / [2v\hbar\Delta W'(R)]. \quad (15)$$

Let us now assume that photon emission actually occurs at R_0 . This corresponds to the system remaining on E_2 with a local probability of $1-p$, so that the overall probability P for emission at R_0 has the form

$$P = \exp\left[-\int_0^{R_0} dR \phi(R)\right] \times \left\{1 - \exp[-\phi(R_0)]\right\}. \quad (16)$$

To generate the entire emission spectrum or lineshape, we must evaluate Eq. (16) for a grid of points in the continuous range of emission frequencies. This equation holds for a single-passage trajectory, as in the reactive system mentioned in the next paragraph. For double-passage it can be readily modified. Improvements on this approach are possible, such as removing the Franck-Condon-type of approximation,⁵¹ but we shall not go into the details here. The above discussion corresponds to a first-order version of a semiclassical theory of spontaneous emission in a collision situation which is capable of treating the molecular dynamics in detail.⁵¹

Our motivation for developing the above theory has come from beautiful experimental results on far-wing emission in the $F + Na_2$ reaction:⁵²



The transition state $FNaNa^{\ddagger*}$ occurs on an excited-state potential surface correlating to $NaF + Na(^2P)$, so that emission to the ground-state potential surface correlating to $NaF + Na(^2S)$ is in the wings associated with the D-line emission. This far-wing emission, whose intensity is about six orders of magnitude less than that of the D-line emission, contains information on the F-Na-Na three-body interactions. [The system can also proceed to the ground-state potential surface via nonradiative non-Born-Oppenheimer coupling, which competes with spontaneous emission.]

The next step in the experiment, which has already been suggested,⁵³ is to apply an intense laser to (17), off-resonant from the D-line. In this case one can envision four electronic-field states as forming a spectrum for spontaneous emission, where the dynamical treatment is similar to that given by Eqs. (14)-(16), except W_1 and W_2 are now replaced by a corresponding pair of electronic-field surfaces.⁵⁴ Since there are six

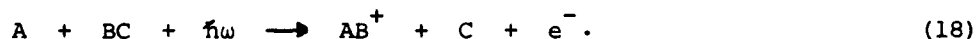
distinct pairs of electronic-field surfaces, in principle an emission spectrum could have six peaks. However, we would be elated to see three peaks corresponding to: 1) the solid vertical line in Fig. 3, 2) the two dashed lines on the left (for an isolated atom these lines coincide precisely) and 3) the dashed line on the right of the solid line. This is similar to what has been observed in studies of the collisional redistribution of light in atom-atom collisions in the presence of a laser field of frequency ω , where the spectrum has one component at ω and two at $\omega \pm (\Delta + \delta)$, Δ being the detuning and δ the ac Stark shift [see Eq. (3)]. There is an active interest in the general topic of line broadening for atom-atom systems in intense laser radiation [see, for examples, Refs. 55-58], and it would be exciting to extend such work to chemical reactions such as (17).

A logical further step in the study of spontaneous emission occurring in molecular collision systems irradiated by intense laser radiation is the delineation of polarization effects.^{56,59,60} The basic idea can be presented in terms of Na + Xe collisions initiated on the $X^2\Sigma$ ground-state potential curve in the presence of laser radiation with a linear polarization. The molecular system can make a (measurable) transition to the $B^2\Sigma$ excited state if (i) the photon energy is resonant with the $X^2\Sigma$ and $B^2\Sigma$ curves at some internuclear separation and (ii) the polarization of the radiation has some component along the direction of the internuclear axis (as the quasimolecule rotates during the collision, this component changes). Let us now presume that a photon has been absorbed such that the molecular system is in the $B^2\Sigma$ state. This state is coupled to two degenerate $A^2\Pi$ states, so that (via nonadiabatic transitions) the $A^2\Pi$ states as well as the $B^2\Sigma$ state become populated. Asymptotically, the $B^2\Sigma$ state correlates to $Na^*(^2P_0) + Xe$ and the $A^2\Pi$ states to $Na^*(^2P_{\pm 1}) + Xe$, where the subscripts refer to projections of electronic angular momentum onto the body-fixed internuclear axis. Transforming to relate these states to their space-fixed counterparts, we can then determine a cross section for populating a specific space-fixed $Na^*(^2P)$ state. When the 2P_0 state fluoresces,

linearly polarized light is emitted, while the $^2P_{+1}$ states decay with circularly polarized light. The inclusion of spin-orbit coupling will highly complicate this picture, adding more coupling among the electronic states and splitting the asymptotic degeneracy of the 2P states. However, the physics is largely unaltered: linearly polarized light goes in, but both linear and circularly polarized light can be emitted. The amount of coherence retention (i.e., amount of linearly polarized light emitted) is an interesting question to be studied for atom-atom systems such as Na + Xe and for reactive systems. The polarization of fluorescence from electronically excited products in the absence of intense laser radiation has been studied,⁶¹⁻⁶³ and the inclusion of intense field effects is an interesting venture.

b. Chemi-Ionization

In Part B we indicated that collisional ionization, known also as chemi-ionization, represents a very feasible avenue for laser-induced effects. The reason for this is that the "resonant" radiative coupling between a discrete molecule state and the electronic continuum can occur over a wide range of internuclear configuration space, so that lower laser intensities are possible as compared to the discrete-discrete radiative coupling depicted in Fig. 2. A natural extension of this idea from the atom-atom systems discussed in Part B.4 is to atom-diatom and chemically reactive systems, e.g.,

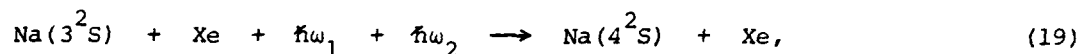


2. Two Radiation Fields

a. Two Different Intense Lasers

For a molecular system in the presence of a single laser, the cross section for a single-photon process is dominated by linear behavior with respect to the laser intensity (up to some threshold where nonlinear behavior begins), while the cross section for a two-photon process is dominated by quadratic behavior. When two different lasers are used (intensity I_i and frequency ω_i , $i=1,2$), a two-photon process ($\hbar\omega_1 + \hbar\omega_2$)

goes as the product $I_1 I_2$. In other words, the behavior is linear with respect to each laser intensity individually. We have verified this with calculations on Na + Xe collisions in the presence of two different lasers,⁶⁴



where $\hbar\omega_1$ and $\hbar\omega_2$ are not resonant with states of atomic sodium. The use of two lasers offers flexibility over a single laser, particularly when one is trying to find resonant points within two (or more) different pairs of potential curves or surfaces, whereby a two-photon process might be more readily achieved than with a single laser.

b. Laser-Magnetic-Field Effects

In the presence of a strong magnetic field, molecular terms other than singlet undergo Zeeman splitting, giving rise to distinct multiple branches. Such branches together with photon-dressing of electronic states by an intense laser yield a multiwell picture, which in turn leads to extra interference effects associated with the nuclear motion. This can result in different dynamical behavior from that found with just the laser.

We have explored this idea in connection with laser-induced predissociation of diatomic molecules.⁶⁵ [In Ref. 65 we were interested in molecules adsorbed on ferromagnetic metals,^{66,67} where the magnetic field can be as high as 10^7 Gauss. However, the formalism developed there can readily be applied to laser-induced gas-phase predissociation in the presence of a strong magnetic field.] Using semiclassical techniques we have calculated total level widths and hence dissociation rates for H_2 , CO and O_2 . In H_2 , for example, the repulsive $^3\Sigma_u^+$ curve is split into three distinct branches by the magnetic field. For H_2 and CO our results show an enhancement up to 20% (for a laser intensity of 10^8 W/cm^2) for laser-magnetic-field induced predissociation over just laser-induced predissociation. For O_2 , however, there is a diminution until the laser intensity reaches 10 TW/cm^2 . In this last case, the magnetic field may be viewed as an agent to sustain bound states in the presence of the laser. The fact that the presence

of a magnetic field causes a diminution rather than an enhancement might be used advantageously; i.e., one may want to use a magnetic field with a laser to block certain undesirable reaction pathways.

c. Transition State Spectroscopy

A possible way to alter the dynamics of chemical reactions without the necessity of high laser intensities is to take advantage of quasibound states which exist when the scattering energy lies close to the energy of a bound state of the molecular system. Effective control of a reaction might proceed from control of the "transition state", and as a step towards understanding this, we suggest the possibility of doing spectroscopy on the quasibound vibronic-field (or rovibronic-field) states formed by a molecular collision in the presence of a laser.^{9,68,69}

To illustrate this idea, let us consider the Xe + F collision system and restrict ourselves to just one covalent curve, say the ground-state one correlating to Xe + F in Fig. 5. We then reverse the sign of the arrow to indicate photon absorption to an excimer state via radiative coupling with a UV laser ($\hbar\omega_1$). The excimer state supports vibrational levels, and let us now envision the application of a second (IR) laser ($\hbar\omega_2$) to induce a transition between two of these levels. The transition is actually between vibronic-field levels (i.e., the vibrational-electronic levels dressed by the first laser), but the energies of the field-free vibrational levels are very close to those of the vibronic-field levels. The separation of the collision partners can take place by several different pathways, the main one involving stimulated emission of a photon of frequency ω_1 . Hence the collision partners gain translational energy of $\hbar\omega_2$, where the second laser induces "laser heating".

The entire process involves the absorption of two photons and the emission of one photon, yet the cross section has the order of magnitude of a single-photon process. This is attributable to the nature of the resonance: the effect of the radiation-induced interaction with the bound states is to hold the molecule together sufficiently long so

that the system can undergo subsequent absorption ($\hbar\omega_2$) and emission ($\hbar\omega_1$). In this sense the first photon absorption event is the "rate-determining step".

An attractive feature is the relatively high total cross section (up to a \AA^2) which can be achieved at fairly low intensities for both lasers (as low as a KW/cm^2). The procedure is to tune the UV laser and the collision energy to maximize the resonance molecular scattering and the Franck-Condon overlap (and also to reduce the slope difference between the potentials at the photon resonance point). In fact, the success in doing this experiment should be better with low intensities rather than high intensities, since the latter would cause too much power broadening of the molecular levels and hence reduce the opportunity for achieving resonance molecular scattering.

We have verified the above statements by means of quantum mechanical calculations within a Fano-type formalism.^{68,69} The absorption lineshapes for the second laser are very sensitive to the choice of frequency of the first laser, which suggests this procedure might be a useful probe of the molecular potentials. Since the overall process is a model for the situation where one laser creates a quasibound collision complex and the other transfers energy within it, a good possibility exists, not just for collisional spectroscopy, but also for enhancing curve-switching probabilities by coupling the relevant nuclear continua to bound electronic states. The ultimate interest is in pushing these ideas for chemical reactions.

III. Surface Processes

A. General Concepts

The studies of gas-phase processes such as described in the previous section are extremely important for understanding the microscopic details of chemical dynamics and reactions. This understanding leads to a better physical interpretation of a variety of important phenomena such as occurring in the upper atmosphere or in specific applications like a gas laser. Nevertheless, most chemistry in the real world occurs in condensed phases, and many practical questions about the utility of basic research seem to center on heterogeneous systems, e.g., gas-solid, gas-liquid and liquid-solid systems. Laser-induced chemistry in condensed phases or heterogeneous systems is not as

well established as in the gas phase, although there seems to be a rapidly increasing effort (especially among gas-phase chemists) to explore how lasers can induce or influence molecular dynamics in condensed phases.

In this article we want to focus on a specific area, namely, laser-induced surface processes, where the surface is an adspecies-substrate (or adsorbate-adsorbent) system in a vacuum or in the presence of a gas, i.e., the gaseous form of the adspecies (the substrate can be a metal, semiconductor or insulator). Strictly speaking the system in a vacuum is not heterogeneous, although it is convenient to regard it as so, in the sense that the adspecies plays the role of a foreign (gaseous-like) species stuck to the solid substrate, with properties usually different than the substrate. This is especially true with physisorption, where binding energies of the adspecies to the substrate are less than 1 eV. Furthermore, in the event of desorption whereby the adspecies breaks away from the surface, we immediately have a gas-solid interface.

The static properties of the adspecies-surface systems have been well studied by a variety of spectroscopic techniques, using an external source of electrons or photons as a probe. The properties studied include the electronic level structure, the site geometry and site selectivity in co-adsorption. The techniques include LEED (low-energy electron diffraction), PES (photoelectron spectroscopy), FEM (field emission microscopy), FIM (field ion microscopy) and synchrotron radiation sources. On the other hand, dynamical processes (with the exception of elastic and inelastic gas-surface scattering) are not as well studied. The dynamical processes of interest generally involve the adspecies and include adsorption, desorption, migration across the surface, diffusion into the bulk and chemical reactions. Our interest in the remainder of this article will be in how the laser can be used as a stimulant of dynamical processes, bearing in mind that it can also be a powerful tool as a probe of static properties. We shall only address several key processes, and for more inclusive reviews we refer the reader to Refs. 1, 10 and 70. [Be aware of the date of a given review when reading it, since the field of laser-surface chemistry is new and changing rapidly.]

Consider a solid surface as represented schematically by a well-ordered lattice in the upper left portion of Fig. 6. A triatomic species is purely gaseous at its furthest distance from the surface. As it approaches the surface, it could enter a state of physisorption, corresponding to binding energies of 0.1 to 1.0 eV. This is indicated by the shallow well in the potential energy diagram. Chemisorption corresponds to binding energies of 1.0 to 5.0 eV or higher, and this is indicated by the deep potential well. One can then envision shining a laser on the chemisorbed adspecies, where the radiation is resonant with a bond within the adspecies (right wiggly arrow) or is resonant with an adsorptive bond which connects the adspecies with the lattice or substrate (left wiggly arrow). Depending on the density of states as a function of frequency of the adspecies-substrate system and the coupling between the adspecies and the surface vibrations (optical and acoustic phonons), the absorbed photon energy could stimulate one (or more) dynamical processes such as desorption by breaking the adsorptive bond, or migration of the adspecies leading to chemical reaction, or the photon energy could be dissipated into the bulk of the substrate with little apparent change on the adspecies. This last option is the least interesting from a chemical point of view, but it is one that cannot be ignored.

A provocative experiment was reported over five years ago.⁷¹ An adspecies-substrate system, where the adspecies was the hydroxyl group (OH) and the substrate was silica (SiO_2), was irradiated in a vacuum cell by a CW CO_2 laser with an intensity of 10 W/cm^2 . The laser frequency was tuned to 950 cm^{-1} to overlap the absorption band associated with Si-OH stretching oscillations. The rate of disappearance of OH was measured by monitoring the disappearance of the spectral line at 3750 cm^{-1} associated with the O-H stretch. The experiment was repeated without the laser by heating the cell to 650°C . Again the OH was observed to disappear, but at a rate much slower than with the laser. Whether the dehydroxylation proceeded via direct desorption of the hydroxyl group or via migration of two hydroxyl groups to form water was not determined. However, the low-power laser was far more effective in inducing dynamical behavior at the surface than conventional

thermal heating. In another experiment involving low-power (30 W/cm^2) CO_2 laser irradiation of silica in an ammonia atmosphere, the rate of decomposition of chemisorbed NH_2 groups was found to be three orders of magnitude larger than that of the corresponding thermal reaction.⁷²

A controversy about the interpretation of the above experiments is whether they involve true selective (nonthermal) excitation or if the laser is simply providing very efficient local heating. This is not an issue which will be resolved in this article, although various points associated with the controversy have been addressed in previous papers.⁷³⁻⁷⁶ These points involve the density of states as a function of frequency, the coupling between the adspecies and the surface phonons (including the role of multiphonon versus single-phonon coupling) and the related question of the lifetime of the states connected with the adsorptive bond. For example, higher lifetimes are better candidates for selective excitation, and one would expect higher lifetimes as the difference between the frequency of the adsorptive bond and those of the surface photons becomes greater. Many of these same points must be addressed in the interpretation of multiphoton excitation of gas-phase molecules.⁷⁷ We would suggest that the issue of selective versus thermal is perhaps not as critical as one might suspect. If dramatic effects can be achieved with local laser heating as compared with thermal oven heating, then the result looks similar to a selective process, even though coherent multiphoton excitation might not actually be taking place. A fair amount of both theoretical and experimental work is still necessary to resolve this controversy (which is most likely very system dependent).

We want to emphasize the low laser intensity ($10\text{-}30 \text{ W/cm}^2$) used in the above experiments to achieve results with IR radiation which resemble those in gas-phase systems with much higher intensities.⁷⁷ An important difference between the surface experiments and the gas-phase experiments is the time scale, which tends to be on the order of seconds to minutes for the former and microseconds or shorter for the latter. One might argue that the longer time scale enables multiphoton excitation with lower intensities.

Support for this idea perhaps comes from ion cyclotron resonance experiments on multi-photon dissociation of gas-phase ions using low-power ($1-100 \text{ W/cm}^2$) CO_2 laser radiation, where an ion can be trapped under nearly collisionless conditions for several seconds.⁷⁸

Interesting laser-surface experiments are not restricted to IR radiation nor to low powers. Furthermore, new chemistry can be achieved by exciting the substrate directly rather than the adspecies. We shall touch on these other types of processes as well as low-power IR-excitation processes in Parts B and C below.

B. Classes of Processes

Depending on the type of laser and adspecies-substrate system, different degrees of freedom will be predominately excited by the incident radiation. It is useful to divide these into nuclear and electronic degrees of freedom, whereby a given process can be viewed as caused by the excitation of certain nuclear degrees of freedom, certain electronic degrees of freedom or some combination of both. We shall discuss such excitations below.

1. Nuclear Degrees of Freedom

In this case we are mainly concerned with IR radiation which vibrationally excites a bond within an adspecies or an adsorptive bond. This vibrational excitation can in turn be transferred to bulk or surface vibrations of the crystal (phonons). In a quantum mechanical description the Hamiltonian can be written as^{10,73-76,79,80}

$$H = H_A + H_B + H_{AB} + H_{ABA} + H_{AF}. \quad (20)$$

It is convenient to use annihilation and creation operators, a_i and a_i^\dagger , separately for the active mode which is laser excited and b_v and b_v^\dagger for the remaining modes. H_A can then be written approximately as

$$H_A = \sum_i \hbar(\omega_i - \epsilon^* a_i^\dagger) a_i^\dagger a_i \quad (21)$$

where ω_i is the vibrational frequency, ϵ^* is an anharmonic correction and the sum runs over lattice sites indexed by i . H_B takes the form

$$H_B = \sum_v \hbar \omega_v b_v^\dagger b_v \quad (22)$$

where ν is an energy level index. H_{AB} is

$$H_{AB} = \sum_i \hbar (F_{i\nu} B_{\{\nu\}} a_i^\dagger + F_{i\nu}^* B_{\{\nu\}}^\dagger a_i) \quad (23)$$

where $F_{i\nu}$ is a multiphonon coupling constant and $B_{\{\nu\}} = \prod b_\nu$. The interaction between the radiation field and the active mode is given to first order as

$$H_{AF} = \sum_i \hbar [V_i(t) (a_i^\dagger + a_i)], \quad (24)$$

where $V_i(t)$ is a matter-field interaction term incorporating the Rabi frequency. H_{AB} represents a coupling from the active mode to the remaining modes, and H_{ABA} represents a feedback mechanism to the active mode.

The information concerning selective and thermal processes and hence the degree of coherent excitation as compared to laser heating is contained in H_{AB} and H_{ABA} . The main obstacle to a realistic calculation is $F_{i\nu}$, and efforts are underway to find reasonable ways to determine this for metal substrates from semiempirical and "almost first-principles" approaches.⁸¹ In the meantime, we have varied parameters to investigate the necessary conditions of selective excitation.⁷⁴⁻⁷⁶ One of the general conclusions, which is not surprising, is that coherent multiphoton excitation leading directly to desorption is more likely for longer lifetimes of the laser-excited mode(s). To be specific, for a laser pumping rate of $5 \times 10^8 \text{ sec}^{-1}$ (or intensity of 30 W/cm^2), a lifetime of a microsecond can result in selective excitation, whereas a lifetime of 10^{-2} microsecond tends to result in thermal heating (this is typically for a metal substrate). The mechanism for laser excitation might also involve features of the adspecies-substrate system which are not explicitly displayed in Eq. (20), such as the image field or surface roughness which have been considered in the interpretation of surface enhanced Raman scattering (SERS) experiments.^{82,83}

One can take a purely classical approach and solve the equations of motion for a model system. We have tried this for a linear chain of silicon atoms (substrate) with an oxygen atom (adspecies) on the end (...Si-Si-Si-Si-O) and a linear chain of lead with hydrogen on the end (...Pb-Pb-Pb-Pb-H).⁸⁴ We were able to determine the band structure

(dispersion relation) and relate it to features of the minimum laser intensity (as a function of the laser frequency) needed for desorption of oxygen or hydrogen. As expected, the absolute minimum occurs when the laser is resonant with the absorptive bond (Si-O), although a relative minimum occurs when the laser is resonant with a Si-Si bond to directly excite an optical phonon of the substrate. Interestingly enough, four to five substrate atoms are sufficient to describe the flow of energy between the adspecies and the substrate, i.e., extending the chain to ten atoms yields no new information.

Extending our studies to a gas-solid interface, we have developed a kinetic model of laser-stimulated desorption utilizing the generalized Langmuir kinetic equation.⁸⁵ With the help of some simple relations, one can evaluate the coverage by the adsorbate and also study the structure of the adsorbent surface by measuring the laser-enhanced partial pressure above the surface.

We have also considered energy transfer in gas-surface scattering in the presence of a laser field using an effective single-phonon model for the surface, where this phonon can be excited by both the incident atom and the laser.⁸⁶ Using classical mechanics we have shown that there exists an interference effect of the gas atoms and the laser radiation in transferring energy to the surface, which can be either constructive or destructive depending on the details of the experimental conditions and the system parameters. Calculations for helium scattering off tungsten, however, have shown that the fraction of interference (with respect to energy transfer from just the gas or just the laser) is only as high as 0.01 for a laser intensity of 10 GW/cm^2 .

2. Electronic Degrees of Freedom

We shall focus our attention here on direct laser excitation of electronic states within the substrate. We are particularly interested in adspecies-semiconductor systems, and as a first step towards treating these we have considered the semiconductor alone. A typical band structure or dispersion relation is displayed in complex crystal momentum space ($k + ik$) for a one-dimensional lattice (e.g., of Si atoms) in Fig. 7.

The real axis lies along a fixed direction in the first Brillouin zone, where the reciprocal lattice constant, g , equals 2π divided by the equilibrium separation between two lattice atoms. The valence band is denoted by V and the conduction band by C , with E_g designating the band gap energy. The special feature of semiconductors which does not occur in metals (or insulators) is the presence of surface states, denoted by S . These states are localized in coordinate space and are functions of the complex momentum.

Using a quantum mechanical model, we have derived an expression for the absorption cross section for a transition from the valence band to the surface band.⁸⁷ The cross section vanishes near $\hbar\omega = E_g/2$ (ω is the laser frequency), where no surface states exist. On the other hand, it tends toward infinity at the extremes $\hbar\omega \rightarrow 0$ and $\hbar\omega \rightarrow E_g$, where $\kappa \rightarrow 0$. This occurs because, at the surface band edges, the charge associated with the surface states becomes more and more delocalized throughout the lattice, until at $\kappa = 0$ the charge is completely delocalized. At this point the surface states become bulk states, and instead of "cross sections" one should really be speaking of absorption "coefficients".

Our main interest is in using a laser to alter the surface charge density. Since the effective charge depth turns out to be $|1/(2\kappa)|$, we wish to excite states with large values of κ . For Si at the maximum κ , the surface charge depth is 1.39 lattice constants (i.e., 1.39 times the equilibrium separation), so that the charge is confined to a region near the top of the surface. Hence we are interested in a laser tuned to a frequency near $E_g/2$ to be an effective controller of surface charge (not precisely where the cross section vanishes but near it). Since the energy gaps for most semiconductors are around 1 eV, the frequency of interest will be in the infrared to low visible region.

The shift in electronic charge and the resultant Coulomb interaction could have a significant effect on the desorption of an adspecies,⁸⁸ particularly for a polar adspecies. When such interaction is repulsive, desorption should be enhanced, and calculations along these lines are in progress.⁸⁹

3. Electronic-Nuclear Degrees of Freedom

In general, any electronic excitation resulting in a dynamical process will also involve a vibrational excitation. For example, in the previous example, since most common semiconductors have indirect band gaps (i.e., the minimum in the conduction band is not located over the maximum in the valence band as in Fig. 7), to excite states in these gaps would require phonon excitation in addition to electronic excitation.

For the case of laser-induced predissociation of a diatomic (or larger) adspecies, the dynamics involves the coupling of electronic and nuclear motion associated with the adspecies. Interactions with surface phonons can modify this coupling. A convenient way to view this process is in terms of photon-phonon-dressed levels, where the electronic levels of the adspecies are dressed simultaneously by the laser field and the surface phonons.⁶⁷

For atom-surface scattering one can capitalize on the concept of photon-dressed or electronic-field states to predict that laser radiation may have appreciable effects on diffraction patterns if the radiation is capable of inducing electronic transitions in the projectile atoms with a large probability.⁹⁰ We estimate, however, that laser intensities would have to be at least a MW/cm^2 for this to occur.

C. Applications

1. Heterogeneous Catalysis

In spite of its very young age, the field of laser-surface chemistry appears to already have exciting prospects for practical applications. The power of solid surfaces as catalysts for numerous chemical reactions is so well established in both research and production that we need not provide references here. The wide use of surface catalysts does not necessarily imply a thorough understanding of how they actually operate, and to a large extent surface catalysis represents black magic, at least from the perspective of a chemical physicist. Admitting a certain ignorance of some of the microscopic details of surface catalysis, we nevertheless take the bold step of asking whether

lasers might be used to enhance a surface-catalytic process. Can a laser and a surface be used in a synergistic fashion to form a catalyst which is better than the surface (or laser) alone? Strictly speaking, the laser will in general not be a catalyst itself since photons will be absorbed.

An experimental example which supports this idea is the bimolecular reaction of NO_2 and C_2H_4 to produce CO_2 .⁹¹ This reaction, carried out in a flask with mixtures of gaseous NO_2 and C_2H_4 at 0.1-1.0 torr, was catalyzed by Pt in the form of a spirally-wound filament. The reaction was repeated in the presence of an Ar^+ laser (488 nm) with a power output of one watt, resulting in a fourfold increase in the production of CO_2 . Another example is the catalytic decomposition of formic acid on Pt, where it was found that irradiation by a CO_2 laser (9.6 μm) with a power of ten watts resulted in an increase of the CO_2/CO product ratio of 50% over that in the absence of the laser.

2. New Reaction Schemes

The combined use of lasers and surfaces might result in a more favorable reaction scheme for making a certain compound. For example, KrF laser (249 nm) irradiation of a sulfur surface in the presence of ethylene vapor yielded ethylene episulfide.⁹² The laser intensity was around a MW/cm^2 , and it is possible that there was multiphoton absorption at the rhombic surface (S_8 molecules), which does absorb at 249 nm. This is believed to be the first synthesis of a simple episulfide directly from elemental sulfur. Two attractive features of this scheme for making ethylene episulfide are: 1) it apparently avoids the production of mercaptans and 2) The reagent elemental sulfide is extremely inexpensive.

3. Microelectronics

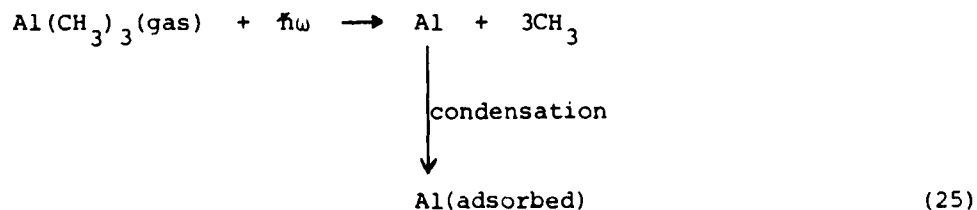
The potential of laser-surface processes for practical applications has received more publicity in connection with microelectronics than any other area. In a recent workshop devoted to the study of the interaction of laser radiation with surfaces for application to microelectronics, representatives from over twenty-five laboratories

(domestic and foreign) reported on results pertinent to this topic.⁹³ The hope is that lasers can enhance the fabrication of very large scale integrated circuits (VLSI).

The most common use of lasers along these lines is in the annealing of semiconductors.⁹⁴ Semiconductors used for integrated circuits must have well-ordered crystal structures, with selected impurities to provide the free electrons (n-type) or "holes" (p-type) that give the semiconductor its precise electrical properties. A popular method of adding controlled amounts of the impurities is ion-implantation. The injection of the ions disrupts the crystal structure, and this damaged material is annealed in a furnace for about an hour at 1,000°C to restore the regular lattice structure. However, due to the long time of this annealing process, unwanted impurities find their way into the material, and furthermore, the semiconductor wafers may become deformed. The laser (fluence $\sim J/cm^2$) has come to the rescue by delivery of heat rapidly to a small area of the material (as small as a few square microns). Since the layer being laser heated is very thin compared to the thickness of the overall material, it also cools quickly and the bulk is not heated significantly.

While the above process of laser annealing is exciting, it does represent a thermal process which is essentially at an engineering stage. However, there are other processes in connection with microelectronics which involve true laser-induced chemistry at a basic research stage.⁹⁵ We shall mention some examples below.

Metal deposition on semiconducting and insulating surfaces has been induced by a frequency-doubled Ar^+ laser (257.2 nm).⁹⁶ The laser was focused onto the surface within a cell containing a few torr of $Al(CH_3)_3$, where Al was then deposited on the surface:



The metal deposits could be localized down to a micron, and by moving the substrate

across the laser one could "write" metal lines at rates of 1000 Å/sec in this lithographic-like procedure. This operation is called laser-induced chemical vapor deposition (LCVD), which has also been studied by using a CO_2 laser to deposit various metals on different substrates.⁹⁷ In these experiments the laser was being used to dissociate metal compounds to form metal atoms which can then be adsorbed. However, the radiation was focused on the substrate, so that evidently the combined action of photodissociation and substrate heating is the mechanism of deposition.

An experiment where this is not the case is one on surface etching by laser-generated free radicals.⁹⁸ Here a CO_2 laser was directed at CF_3Br gas above a silicon surface coated with SiO_2 . Photodissociation resulted in CF_3 and Br radicals which reacted with the SiO_2 to form gaps in the coating. Since the radiation was aimed parallel to the substrate, it is believed that there is probably no laser-surface interaction. Surface etching, however, has also been carried out by shining a laser directly on a substrate, and at the same time photolyzing a gas to create radicals which react with the surface in the etching process.⁹⁹

The main message to be conveyed is that some of the most exciting experiments in the area of microelectronics are based on laser-induced chemistry, either in the gas phase above a substrate or at a gas-surface interface. Hence, basic research on laser-surface molecular rate processes has a direct line to payoffs in applied science.

Acknowledgments

The author is indebted to the excellent Research Associates who have recently been or are presently members of his group for numerous, extensive, stimulating conversations, particularly the names appearing as co-authors on Refs. 1, 8, 9, 10, 19 and 74. This work was supported in part by the Air Force Office of Scientific Research (AFSC), United States Air Force, under Contract No. F49620-78-C-0005, the Office of Naval Research and the National Science Foundation under Grant No. CHE-8022874. The United States Government is authorized to reproduce and distribute reprints for governmental purposes notwithstanding any copyright notation hereon. The author acknowledges the Camille and Henry Dreyfus Foundation for a Teacher-Scholar Award (1975-82).

References

1. T. F. George, A. C. Beri, K. S. Lam and J. Lin, "Laser Photochemistry" in Laser Applications, Vol. 5, ed. by J. F. Ready (Academic, New York, 1981), in press.
2. T. F. George, Opt. Eng. **18**, 167 (1979).
3. T. F. George, ed., Special Issue on "Laser Applications to Chemistry", Opt. Eng. **19**, 1-112 (1980).
4. A. H. Zewail, V. S. Letokhov, R. N. Zare, R. B. Bernstein, Y. T. Lee and Y. R. Shen in A Special Issue on "Laser Chemistry", Physics Today **33** (11), 25-59 (1980).
5. P. L. DeVries, K. S. Lam and T. F. George in Electronic and Atomic Collisions, ed. by N. Oda and K. Takayanagi (North-Holland, Amsterdam, 1980), pp. 683-695.
6. S. I. Yakovlenko, Sov J. Quantum Electron. **8**, 151 (1978).
7. F. H. Mies in Theoretical Chemistry: Advances and Perspectives, Vol. 6B, ed. by D. Henderson (Academic, New York, 1981), pp. 127-198.
8. T. F. George, I. H. Zimmerman, P. L. DeVries, J. M. Yuan, K. S. Lam, J. C. Bellum, H. W. Lee, M. S. Slutsky and J. Lin in Chemical and Biochemical Applications of Lasers, Vol. IV, ed. by C. B. Moore (Academic, New York, 1979), pp. 253-354.
9. T. F. George, I. H. Zimmerman, P. L. DeVries, J. M. Yuan, K. S. Lam, D. K. Bhattacharyya and M. Hutchinson, J. Phys. Chem., in press.
10. T. F. George, J. Lin, K. S. Lam and C. Chang, Opt. Eng. **19**, 100 (1980).
11. G. C. Lie, J. Chem. Phys. **60**, 2995 (1974). See also R. N. Siles and T. A. Cool, J. Chem. Phys. **65**, 117 (1976).
12. C. F. Bender and E. R. Davidson, J. Chem. Phys. **49**, 4989 (1968).
13. R. Hefferlin, J. Quant. Spectrosc. Radiat. Transfer **16**, 1101 (1976).
14. T. G. Slanger and G. Black, J. Chem. Phys. **64**, 219 (1976).
15. P. J. Hay and T. H. Dunning, Jr., J. Chem. Phys. **69**, 2209 (1978). See also A. L. Smith, I. Messing and B. Galernt, J. Chem. Phys. **73**, 2618 (1980).
16. B. Laskowski, S. R. Langhoff and J. R. Stallcop, J. Chem. Phys. **75**, 815 (1981).
17. P. L. DeVries, C. Chang, T. F. George, B. Laskowski and J. R. Stallcop, Phys. Rev. A **22**, 545 (1980).
18. N. M. Kroll and K. M. Watson, Phys. Rev A **13**, 1018 (1976).
19. T. F. George, I. H. Zimmerman, J. M. Yuan, J. R. Laing and P. L. DeVries, Acc. Chem. Res. **10**, 449 (1977).
20. P. L. DeVries, K. S. Lam and T. F. George, Int. J. Quantum Chem. Symp. No. 13, 541 (1979).

21. I. H. Zimmerman, T. F. George, J. R. Stallcop and B. C. F. M. Laskowski, Chem. Phys. 49, 59 (1980).
22. I. H. Zimmerman, J. M. Yuan and T. F. George, J. Chem. Phys. 66, 2638 (1977).
23. P. L. DeVries and T. F. George, Mol. Phys. 36, 151 (1978).
24. J. M. Yuan, J. R. Laing and T. F. George, J. Chem. Phys. 66, 1107 (1977).
25. R. W. Falcone, W. R. Green, J. C. White, J. F. Young and S. E. Harris, Phys. Rev. A 15 1333 (1977); S. E. Harris and J. F. Young in Radiation Energy Conversion in Space, ed. by K. W. Billman, Prog. Astron. Aeron. 61, 583 (1978); S. E. Harris and J. C. White, IEEE J. Quantum Electron. QE-13, 972 (1977).
26. Ph. Cahuzac and P. E. Toschek, Phys. Rev. Lett. 40, 1087 (1978); C. Bréchnignac, Ph. Cahuzac and P. E. Toschek, Phys. Rev. A 21, 1969 (1980).
27. J. Lukasik and S. C. Wallace, Phys. Rev. Lett. 47, 240 (1981). [A theoretical study of vibrational energy exchange in CO + NO + $h\nu$ collisions has been reported by M. Mohan, J. Chem. Phys. 75, 1772 (1981).]
28. P. Hering, P. R. Brooks, R. F. Curl, Jr., R. S. Hudson and R. S. Lowe, Phys. Rev. Lett. 44, 687 (1980).
29. B. E. Wilcomb and R. Burnham, J. Chem. Phys. 74, 6784 (1981).
30. M. K. Bullitt, C. H. Fisher and J. L. Kinsey, J. Chem. Phys. 60, 478 (1974).
31. J. H. Waters and H. B. Gray, J. Amer. Chem. Soc. 85, 825 (1963).
32. P. Polak-Dingels, J.-F. Delpech and J. Weiner, Phys. Rev. Lett. 44, 1663 (1980); J. Weiner and P. Polak-Dingels, J. Chem. Phys. 74, 508 (1981); A. v. Hellfeld, J. Caddick and J. Weiner, Phys. Rev. Lett. 40, 1369 (1978).
33. F. Roussel, B. Carré, P. Breger and G. Spiess, J. Phys. B: At. Mol. Phys. 14, L313 (1981).
34. C. Bréchnignac, Ph. Cahuzac and A. Debarré, J. Phys. B: At. Mol. Phys. 13, L383 (1980).
35. J. Weiner, J. Chem. Phys. 72, 2856 (1980).
36. M. H. Nayfeh, Phys. Rev. A 16, 927 (1977).
37. J. C. Bellum and T. F. George, J. Chem. Phys. 68, 134 (1978).
38. J. C. Bellum and T. F. George, J. Chem. Phys. 70, 5059 (1979).
39. A. Weingartshofer, J. K. Holmes, G. Caudle, E. M. Clarke and H. Krüger, Phys. Rev. Lett. 39, 269 (1977).
40. J. M. Yuan and T. F. George, J. Chem. Phys. 70, 990 (1979).
41. A. E. Orel and W. H. Miller, J. Chem. Phys. 70, 4393 (1979).

42. Sr. K. Duffy and J. M. Yuan, to be published.
43. A. M. Naqvi and S. P. Talwar, Monthly Notices Roy. Astron. Soc. 117, 463 (1957).
44. J. C. Light and A. Altenberger-Siczek, J. Chem. Phys. 70, 4108 (1979).
45. A. M. F. Lau, Phys. Rev. Lett. 43, 1009 (1978); *ibid.*, Phys. Rev. A 22, 614 (1980).
46. N. M. Kroll and K. M. Watson, Phys. Rev. A 5, 1883 (1972).
47. B. K. Deka, P. E. Dyer, D. J. James and S. A. Ramsden, Opt. Commun. 19, 292 (1976).
48. H. W. Lee, P. L. DeVries, I. H. Zimmerman and T. F. George, Mol. Phys. 36, 1693 (1978). For further work on multimodes and linewidths, see H. W. Lee, P. L. DeVries and T. F. George, J. Chem. Phys. 69, 2596 (1978).
49. P. L. DeVries and T. F. George, Phys. Rev. A 18, 1751 (1978); *ibid.*, Mol. Phys. 38, 561 (1979).
50. A similar approach in connection with Penning ionization has been carried out by W. H. Miller, J. Chem. Phys. 52, 3563 (1970), and the extension to laser-induced Penning ionization by J. S. Dahler, R. E. Turner and S. E. Nielsen, J. Phys. Chem., in press.
51. K. S. Lam and T. F. George, J. Chem. Phys. 76, in press (1982).
52. P. Arrowsmith, F. E. Baroszek, S. H. P. Bly, T. Carrington, Jr., P. E. Charters and J. C. Polanyi, J. Chem. Phys. 73, 5895 (1980).
53. J. C. Polanyi, Faraday Disc. Chem. Soc. 67, 129 (1979).
54. K. S. Lam, I. H. Zimmerman, J. M. Yuan, J. R. Laing and T. F. George, Chem. Phys. 26, 455 (1977).
55. J. L. Carlsten, A. Szöke and M. G. Raymer, Phys. Rev. A 15, 1029 (1977); M. G. Raymer, J. L. Carlsten and G. Pichler, J. Phys. B: At. Mol. Phys. 12, L119 (1979).
56. K. Burnett, J. Cooper, J. R. Ballagh and E. W. Smith, Phys. Rev. A 22, 2005, 2027, 2044 (1980); P. Thomann, K. Burnett and J. Cooper, Phys. Rev. Lett. 45, 1325 (1980).
57. M. G. Payne, V. E. Anderson and J. E. Turner, Phys. Rev. A 20, 1032 (1979).
58. G. Nienhuis and F. Schuller, J. Phys. B: At. Mol. Phys. 13, 2205 (1980).
59. J. Light and A. Szöke, Phys. Rev. A 18, 1363 (1978).
60. P. R. Berman, Phys. Rev. A 22, 1838 (1980).
61. C. D. Jonah, R. N. Zare and Ch. Ottinger, J. Chem. Phys. 56, 263 (1972).
62. M. G. Prisant, C. T. Rettner and R. N. Zare, J. Chem. Phys. 75, 2222 (1981).
63. R. J. Hennessy, Y. Ono and J. P. Simons, Mol. Phys., in press.

64. P. L. DeVries, C. Chang, T. F. George, B. Laskowski and J. R. Stallcop, Phys. Rev. A 22, 545 (1980).
65. D. K. Bhattacharyya, K. S. Lam and T. F. George, J. Chem. Phys. 75, 203 (1981). For a study of laser-induced predissociation using photon-dressed electronic states (in the absence of a magnetic field), see A. D. Bandrauk and M. Sink, J. Chem. Phys. 74, 1110 (1981).
66. M. P. Das and J. Mahanty, Chem. Phys. Lett. 67, 142 (1979).
67. J. Lin and T. F. George, Surface Sci. 107, 417 (1981).
68. M. Hutchinson and T. F. George, Phys. Lett. 82A, 119 (1981).
69. M. Hutchinson and T. F. George, J. Chem. Phys., submitted.
70. N. V. Karlov and A. M. Prokhorov, Sov. Phys. Usp. 20, 721 (1977).
71. M. S. Djidjoev, R. V. Khokhlov, A. V. Kiselev, V. I. Lygin, V. A. Namiot, A. I. Osipov, V. I. Panchenko and B. I. Provotorov in Tunable Lasers and Applications, ed. by A. Mooradian, T. Jaeger and P. Stokseth (Springer, Berlin, 1976), pp. 100-107.
72. M. S. Dzhydzhoev, A. J. Osipov, V. Ya. Panchenko, V. T. Planonenko, R. V. Khokhlov and K. V. Shaitan, Sov. Phys. JETP 47, 684 (1978).
73. J. Lin and T. F. George, J. Phys. Chem. 72, 2554 (1980).
74. J. Lin, A. C. Beri, M. Hutchinson, W. C. Murphy and T. F. George, Phys. Lett. 79A, 233 (1980).
75. J. Lin and T. F. George, Surf. Sci. 100, 381 (1980).
76. J. Lin and T. F. George, J. Phys. Chem. 84, 2957 (1980).
77. See V. S. Letokhov in Ref. 4.
78. R. L. Woodin, D. S. Bomse and J. L. Beauchamp in Chemical and Biochemical Applications of Lasers, Vol. IV, ed. by C. B. Moore (Academic, New York, 1979), pp. 355-388.
79. M. S. Slutsky and T. F. George, Chem. Phys. Lett. 57, 473 (1978).
80. M. S. Slutsky and T. F. George, J. Chem. Phys. 70, 1231 (1979).
81. A. C. Beri and T. F. George, manuscript in preparation.
82. H. Metiu, personal communication.
83. F. W. King, R. P. Van Duyne and G. C. Schatz, J. Chem. Phys. 69, 4472 (1978); S. Elfrima and H. Metiu, Chem. Phys. Lett. 60, 59 (1978); P. R. Hilton and D. W. Oxtoby, J. Chem. Phys. 72, 6346 (1980); A. Nitzan and L. E. Brus, J. Chem. Phys. 75, 2205 (1981).
84. W. C. Murphy and T. F. George, Surface Sci. 102, L46 (1981).
85. J. Lin and T. F. George, Chem. Phys. Lett. 66, 5 (1979).
86. H. W. Lee and T. F. George, J. Chem. Phys. 70, 4220 (1979).

87. W. C. Murphy and T. F. George, Surface Sci., submitted.
88. This is under experimental investigation by E. Weitz and co-workers.
89. W. C. Murphy and T. F. George, unpublished.
90. H. W. Lee and T. F. George, Theoret. Chim. Acta (Berl.) 53, 193 (1979).
91. M. E. Umstead, L. D. Talley, D. E. Tevault and M. C. Lin, Opt. Eng. 19, 94 (1980).
92. D. R. Betteridge and J. T. Yardley, Chem. Phys. Lett. 62, 570 (1979).
93. Workshop on the Interaction of Laser Radiation with Surfaces for Application to Microelectronics, Massachusetts Institute of Technology, May 4-5, 1981.
94. D. H. Auston, W. L. Brown and G. K. Celler, Bell Laboratories Record, July/August, 1979, pp. 187-191.
95. Physics Today 33 (10), 21-22 (1980).
96. T. F. Deutsch, D. J. Ehrlich and R. M. Osgood, Jr., Appl. Phys. Lett. 35, 175 (1979).
97. S. D. Allen and M. Bass, J. Vac. Sci. Technol. 16, 431 (1979).
98. J. I. Steinfeld, T. G. Anderson, C. Reiser, B. R. Denison, L. D. Hartsough and J. R. Hollahan, J. Electrochem. Soc. 127, 514 (1980).
99. D. J. Ehrlich, R. M. Osgood, Jr. and T. F. Deutsch, Appl. Phys. Lett. 38, 1018 (1981).

Figure Captions

1. Representative illustration of the applications of lasers to studies of bimolecular chemical reactions, where the circle denotes the interaction region. The first two cases (a) and (b) correspond to laser radiation ($\hbar\omega$ and $\hbar\omega_1$, where ω and ω_1 are frequencies) of moderate or weak intensity; (a) is laser selection of an initial energy level of the reactant BC, and (b) is the spectroscopic analysis of the product AB ($\hbar\omega_2$ corresponds to emission at a different frequency). For high enough intensity the radiation can interact directly with the reaction dynamics, which is the last case (c).
2. (a) The energy, E , of two field-free potential energy curves, W_1 and W_2 , plotted as a function of the internuclear separation, R . The vertical line corresponds to a laser photon of energy $\hbar\omega$ in resonance with the curves at $R = R_0$.
(b) The electronic-field curves, E_1 and E_2 , resulting from (a).
3. Generalization of Fig. 2, where E_2 and E_3 correspond to E_1 and E_2 , respectively, in Fig. 2 with $N=1$. The vertical lines correspond to spontaneous emission, which is addressed in Part D of Section II.
4. Schematic drawing of the field-free potential energy surfaces, W_1 and W_2 , including spin-orbit coupling, along a reaction coordinate, s , for the $F + H_2$ reactive system. The photon energy from the Nd:glass laser is indicated by the vertical line, where the double-ended arrow indicates both absorption (up) and stimulated emission (down).
5. Schematic illustration of a two-photon radiative quenching process.
6. Schematic illustration of physisorption and chemisorption in an adspecies/substrate system.
7. Dispersion relation in complex crystal momentum space ($k + ik$) for a finite linear semiconductor chain. The valence, surface and conduction bands are labeled V, S and C, respectively, and E_g is the band gap energy.

Fig. 1

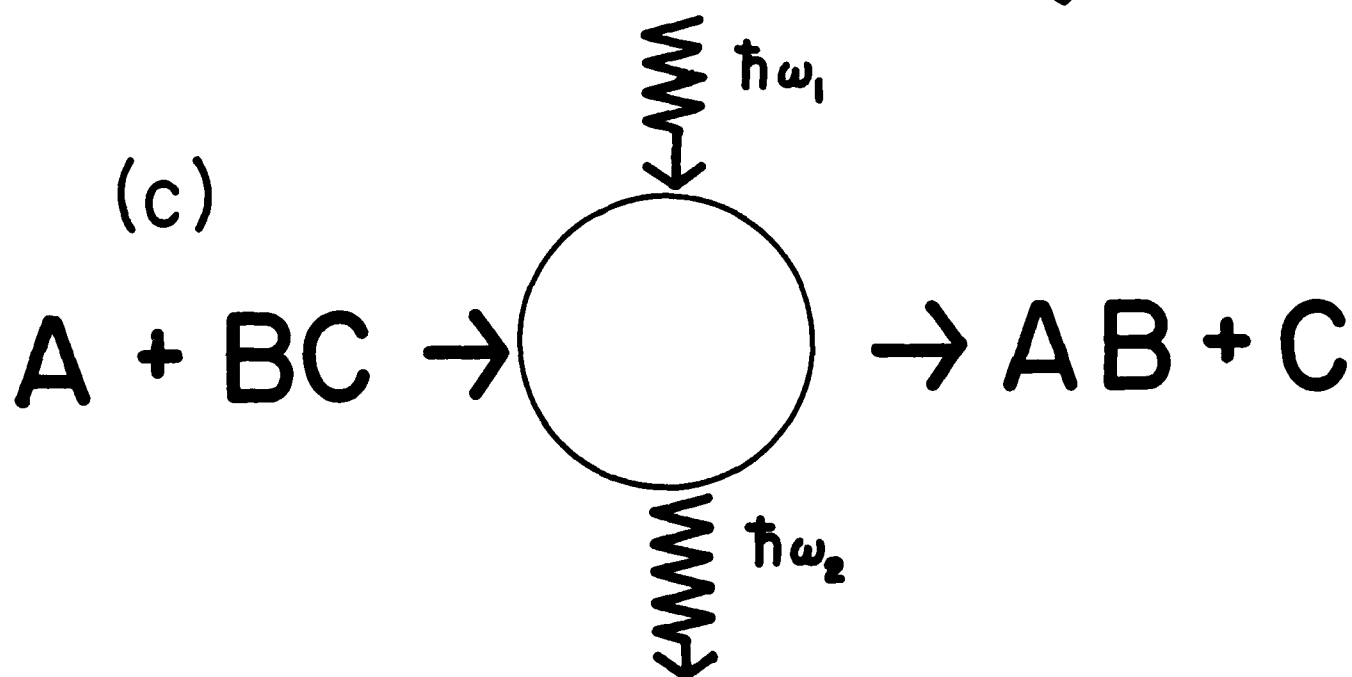
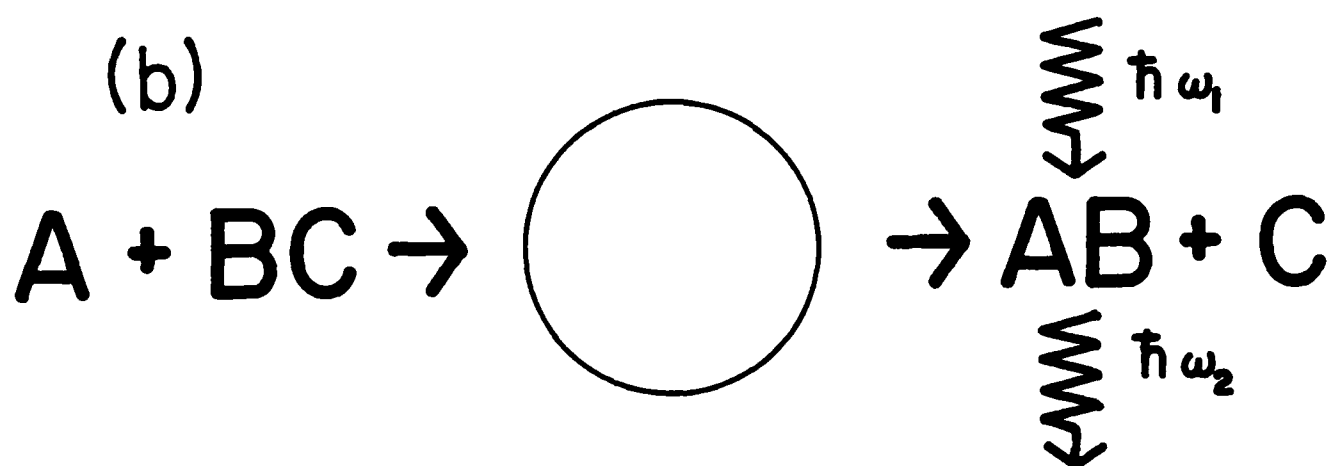
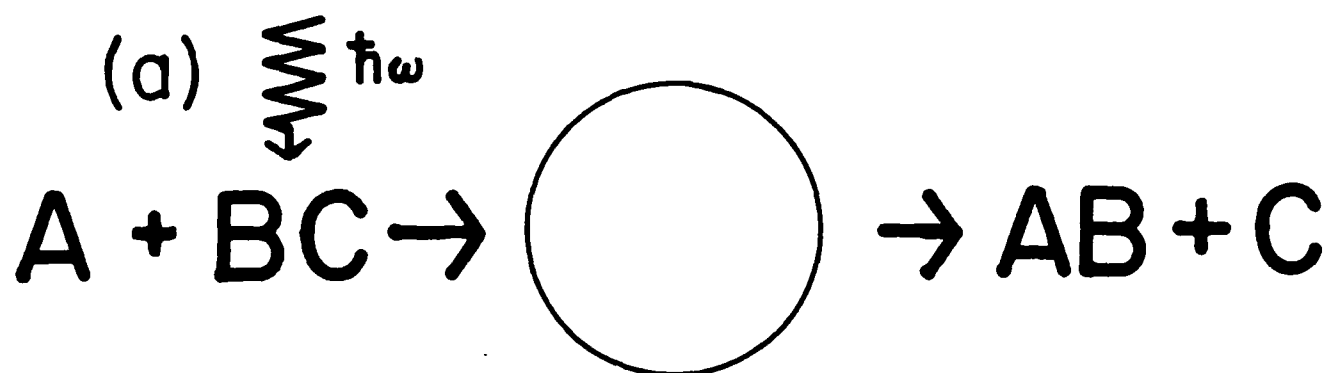


Fig. 2

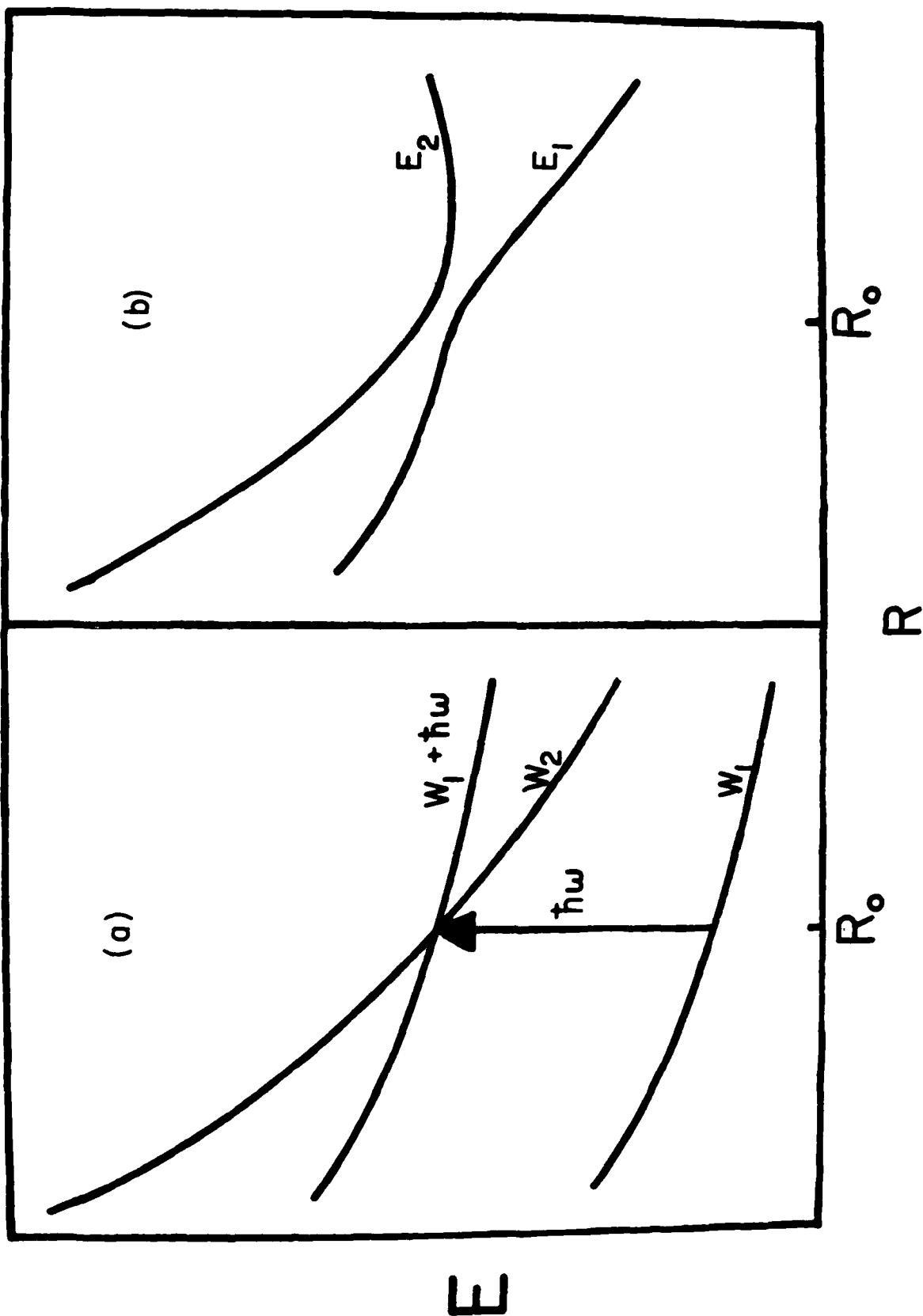


Fig. 3

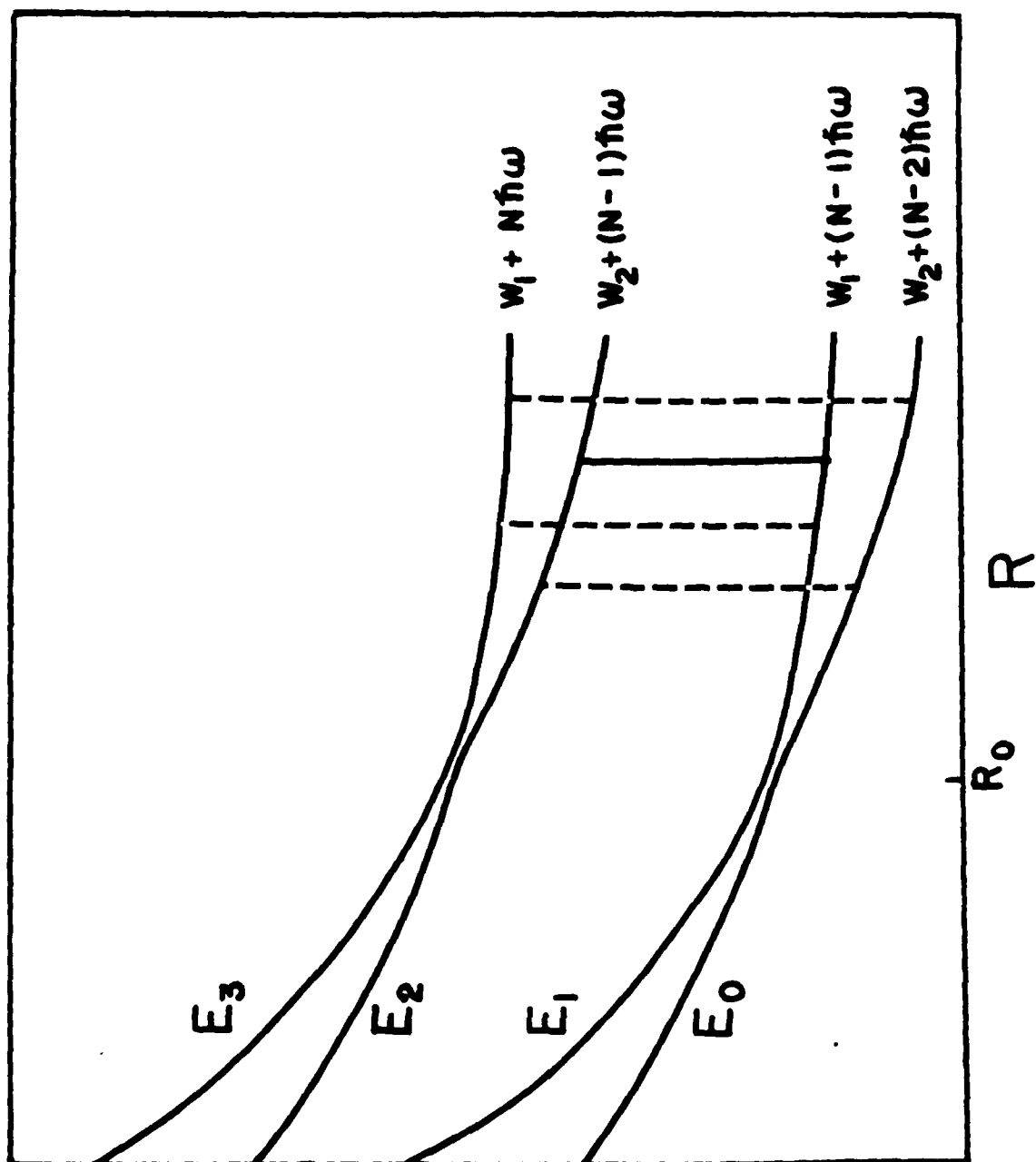


Fig. 4

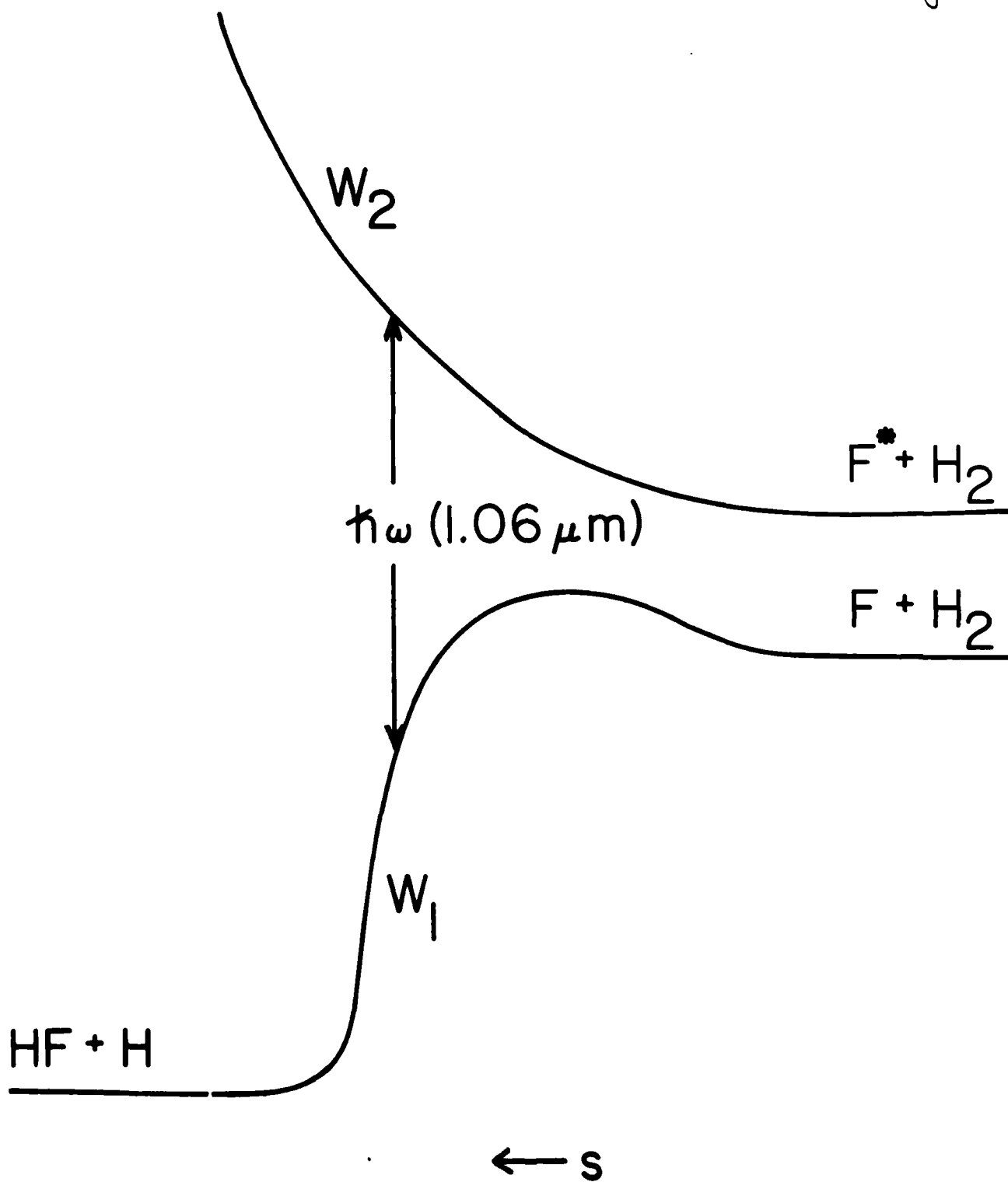


Fig 5

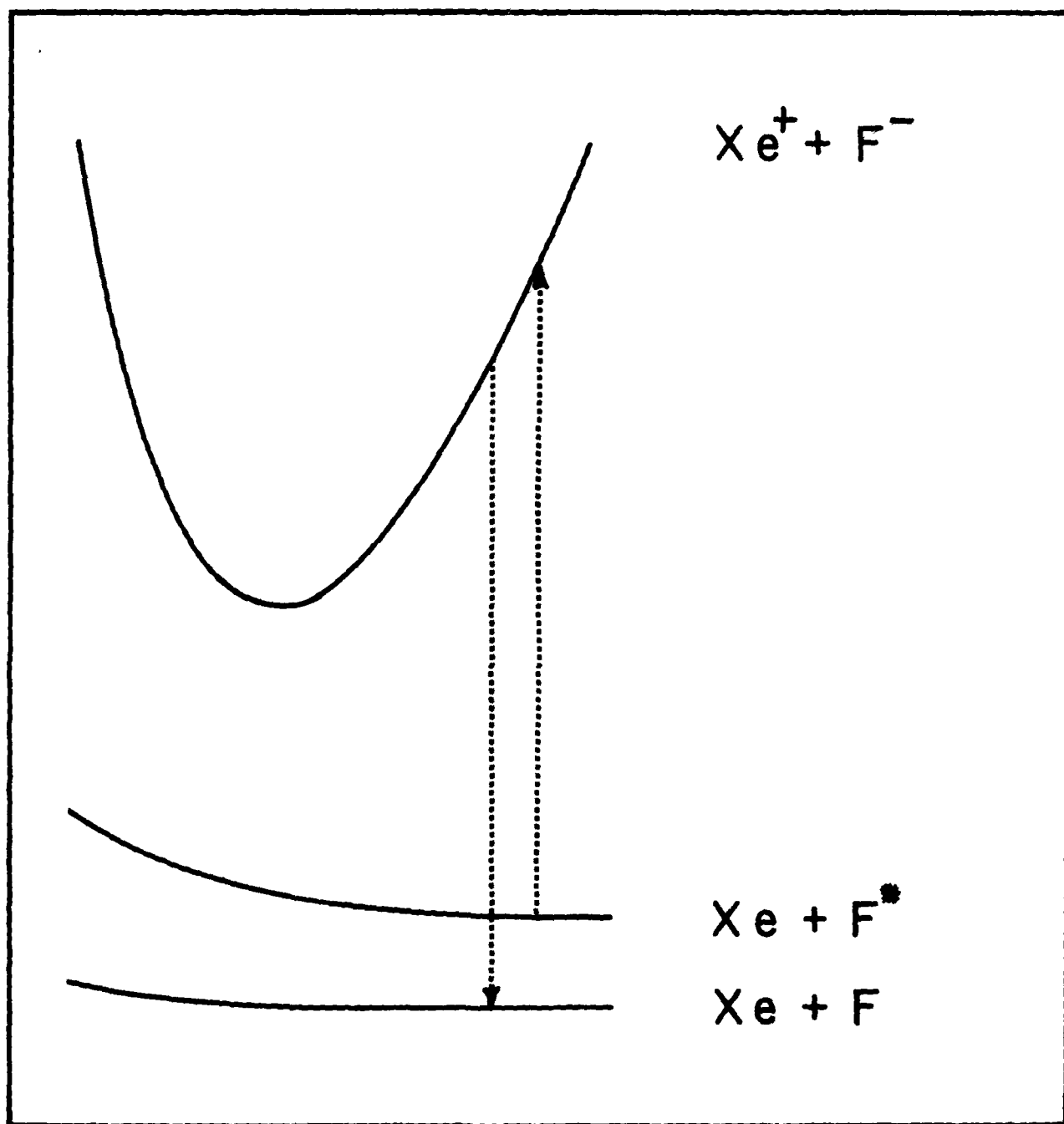


Fig. 6

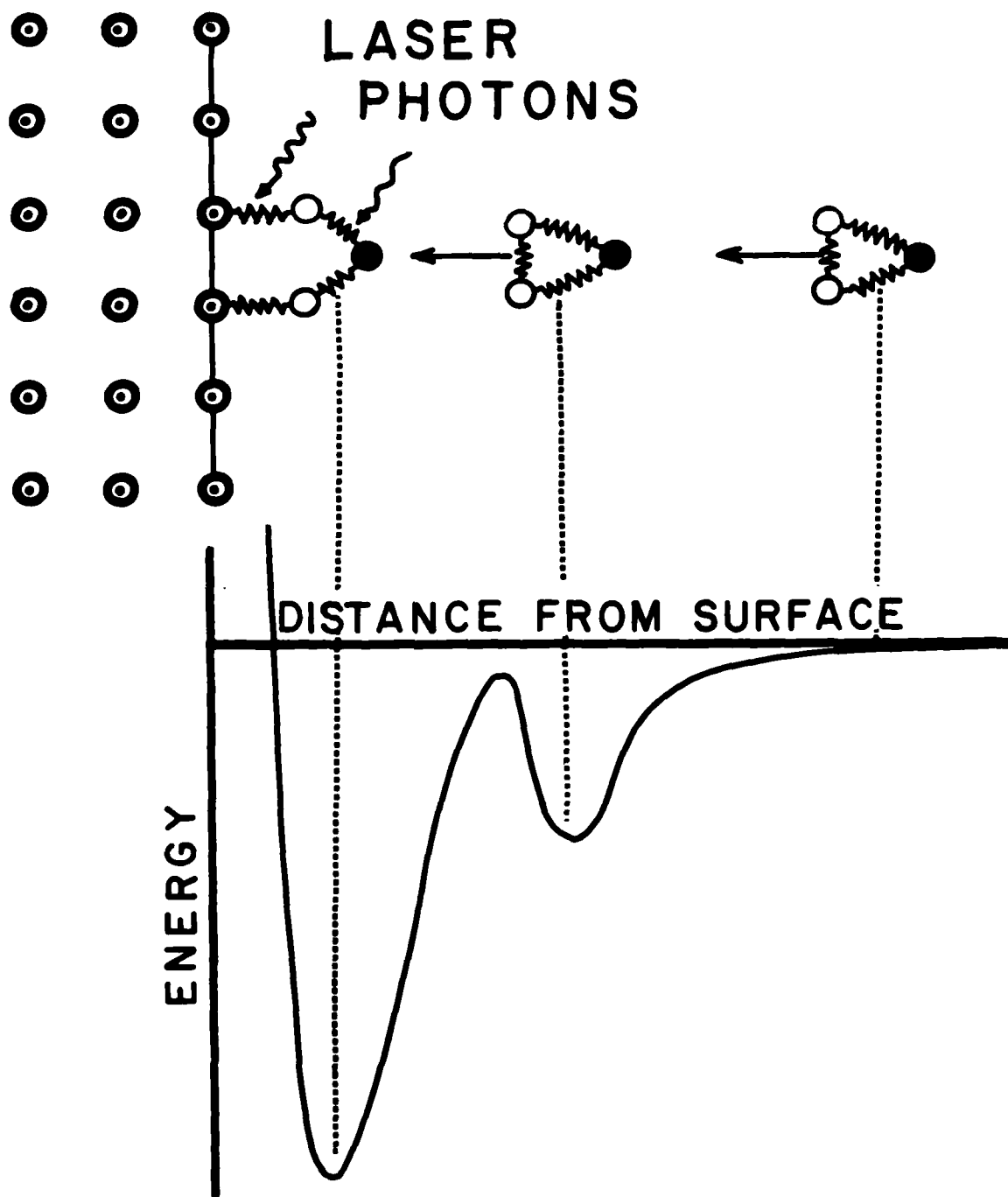
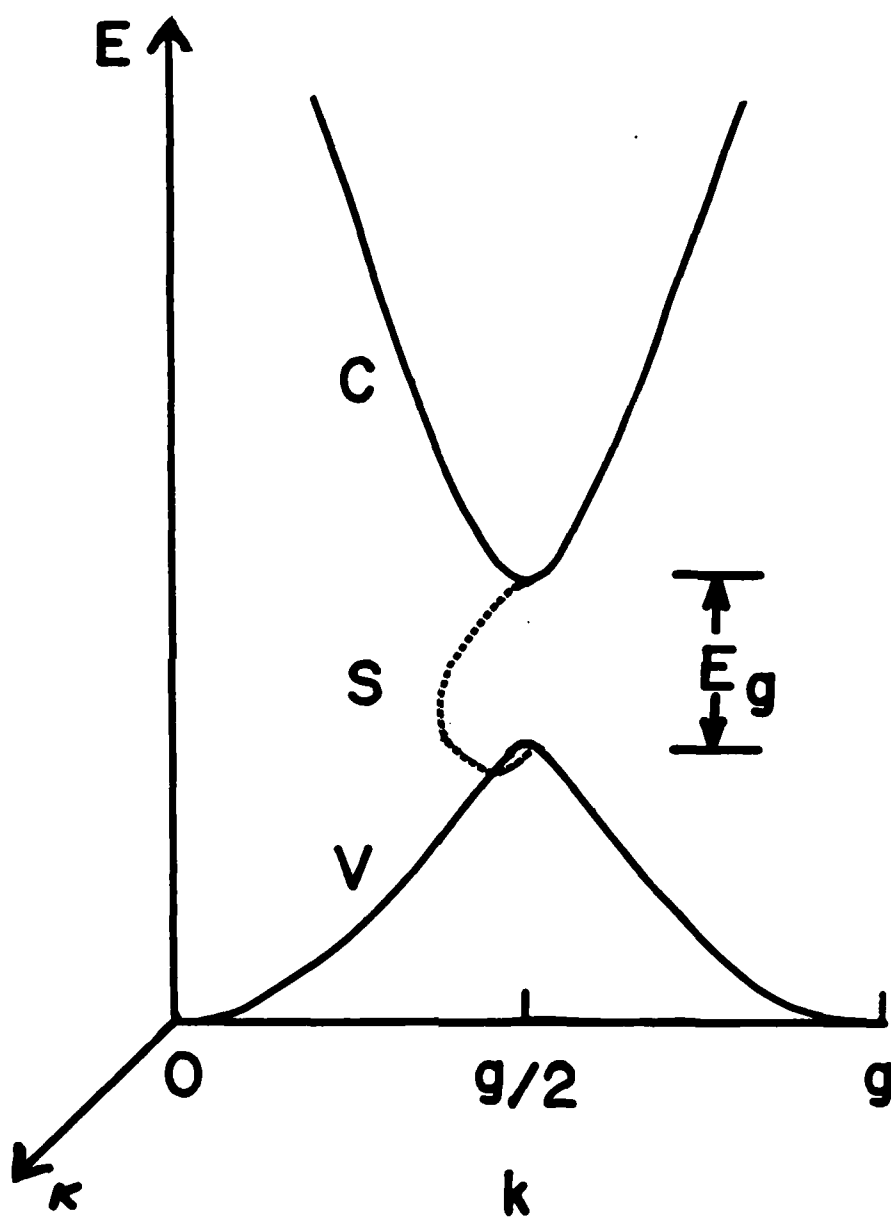


Fig. 7



TECHNICAL REPORT DISTRIBUTION LIST, GEN

	<u>No.</u> <u>Copies</u>		<u>No.</u> <u>Copies</u>
Office of Naval Research Attn: Code 472 800 North Quincy Street Arlington, Virginia 22217	2	U.S. Army Research Office Attn: CRD-AA-IP P.O. Box 12211 Research Triangle Park, N.C. 27709	1
ONR Western Regional Office Attn: Dr. R. J. Marcus 1030 East Green Street Pasadena, California 91106	1	Naval Ocean Systems Center Attn: Mr. Joe McCartney San Diego, California 92152	1
ONR Eastern Regional Office Attn: Dr. L. H. Peebles Building 114, Section D 666 Summer Street Boston, Massachusetts 02210	1	Naval Weapons Center Attn: Dr. A. B. Amster, Chemistry Division China Lake, California 93555	1
Director, Naval Research Laboratory Attn: Code 6100 Washington, D.C. 20390	1	Naval Civil Engineering Laboratory Attn: Dr. R. W. Drisko Port Hueneme, California 93401	1
The Assistant Secretary of the Navy (RE&S) Department of the Navy Room 4E736, Pentagon Washington, D.C. 20350	1	Department of Physics & Chemistry Naval Postgraduate School Monterey, California 93940	1
Commander, Naval Air Systems Command Attn: Code 3100 (H. Rosenwasser) Department of the Navy Washington, D.C. 20360	1	Scientific Advisor Commandant of the Marine Corps (Code RD-1) Washington, D.C. 20380	1
Defense Technical Information Center Building 5, Cameron Station Alexandria, Virginia 22314	12	Naval Ship Research and Development Center Attn: Dr. G. Bosmajian, Applied Chemistry Division Annapolis, Maryland 21401	1
Dr. Fred Saalfeld Chemistry Division, Code 6100 Naval Research Laboratory Washington, D.C. 20375	1	Naval Ocean Systems Center Attn: Dr. S. Yamamoto, Marine Sciences Division San Diego, California 91032	1
Dr. David L. Nelson Chemistry Program Office of Naval Research 800 North Quincy Street Arlington, Virginia 22217	1	Mr. John Boyle Materials Branch Naval Ship Engineering Center Philadelphia, Pennsylvania 19112	1

TECHNICAL REPORT DISTRIBUTION LIST, 056

	<u>No. Copies</u>		<u>No. Copies</u>
Dr. G. A. Somorjai Department of Chemistry University of California Berkeley, California 94720	1	Dr. C. P. Flynn Department of Physics University of Illinois Urbana, Illinois 61801	1
Dr. L. N. Jarvis Surface Chemistry Division 4555 Overlook Avenue, S.W. Washington, D.C. 20375	1	Dr. W. Kohn Department of Physics University of California (San Diego) LaJolla, California 92037	1
Dr. J. B. Hudson Materials Division Rensselaer Polytechnic Institute Troy, New York 12181	1	Dr. R. L. Park Director, Center of Materials Research University of Maryland College Park, Maryland 20742	1
Dr. John T. Yates Department of Chemistry University of Pittsburgh Pittsburgh, Pennsylvania 15260	1	Dr. W. T. Peria Electrical Engineering Department University of Minnesota Minneapolis, Minnesota 55455	1
Dr. Theodore E. Madey Surface Chemistry Section Department of Commerce National Bureau of Standards Washington, D.C. 20234	1	Dr. Chia-wei Woo Department of Physics Northwestern University Evanston, Illinois 60201	1
Dr. J. M. White Department of Chemistry University of Texas Austin, Texas 78712	1	Dr. D. C. Mattis Polytechnic Institute of New York 333 Jay Street Brooklyn, New York 11201	1
Dr. Keith H. Johnson Department of Metallurgy and Materials Science Massachusetts Institute of Technology Cambridge, Massachusetts 02139	1	Dr. Robert M. Hexter Department of Chemistry University of Minnesota Minneapolis, Minnesota 55455	1
Dr. J. E. Demuth IBM Corporation Thomas J. Watson Research Center P.O. Box 218 Yorktown Heights, New York 10598	1	Dr. R. P. Van Duyne Chemistry Department Northwestern University Evanston, Illinois 60201	1

TECHNICAL REPORT DISTRIBUTION LIST, 056

	<u>No. Copies</u>		<u>No. Copies</u>
Dr. S. Sibener Department of Chemistry James Franck Institute 5640 Ellis Avenue Chicago, Illinois 60637	1	Dr. Martin Fleischmann Department of Chemistry Southampton University Southampton SO9 5NH Hampshire, England	1
Dr. M. G. Lagally Department of Metallurgical and Mining Engineering University of Wisconsin Madison, Wisconsin 53706	1	Dr. J. Osteryoung Chemistry Department State University of New York at Buffalo Buffalo, New York 14214	1
Dr. Robert Gomer Department of Chemistry James Franck Institute 5640 Ellis Avenue Chicago, Illinois 60637	1	Dr. G. Rubloff I.B.M. Thomas J. Watson Research Center P. O. Box 218 Yorktown Heights, New York 10598	1
Dr. R. G. Wallis Department of Physics University of California, Irvine Irvine, California 92664	1	Dr. J. A. Gardner Department of Physics Oregon State University Corvallis, Oregon 97331	1
Dr. D. Ramaker Chemistry Department George Washington University Washington, D.C. 20052	1	Dr. G. D. Stein Mechanical Engineering Department Northwestern University Evanston, Illinois 60201	1
Dr. P. Hansma Chemistry Department University of California, Santa Barbara Santa Barbara, California 93106	1	Dr. K. G. Spears Chemistry Department Northwestern University Evanston, Illinois 60201	1
Dr. P. Hendra Chemistry Department Southampton University England SO9JNH	1	Dr. R. W. Plummer University of Pennsylvania Department of Physics Philadelphia, Pennsylvania 19104	1
Professor P. Skell Chemistry Department Pennsylvania State University University Park, Pennsylvania 16802	1	Dr. E. Yeager Department of Chemistry Case Western Reserve University Cleveland, Ohio 41106	2
Dr. J. C. Hemminger Chemistry Department University of California, Irvine Irvine, California 92717	1	Professor D. Hercules University of Pittsburgh Chemistry Department Pittsburgh, Pennsylvania 15260	1

TECHNICAL REPORT DISTRIBUTION LIST, 056

No.
Copies

Professor N. Winograd
The Pennsylvania State University
Department of Chemistry
University Park, Pennsylvania 16802 1

Professor I. F. George
The University of Rochester
Chemistry Department
Rochester, New York 14627 1

Professor Dudley R. Herschbach
Harvard College
Office for Research Contracts
1350 Massachusetts Avenue
Cambridge, Massachusetts 02138 1

Professor Horia Metiu
University of California,
Santa Barbara
Chemistry Department
Santa Barbara, California 93106 1

Professor A. Steckl
Rensselaer Polytechnic Institute
Department of Electrical and
Systems Engineering
Integrated Circuits Laboratories
Troy, New York 12181 1

Professor R. D. Archer
University of Massachusetts
Chemistry Department
Amherst, Massachusetts 01003 1

Dr. A. C. Pastor
Hughes Research Laboratories
3011 Malibu Canyon Road
Malibu, California 90265 1

DAT
ILM